Journal of Asian Earth Sciences 62 (2013) 438–462

Contents lists available at SciVerse ScienceDirect

Journal of Asian Earth Sciences

journal homepage: www.elsevier.com/locate/jseaes

Mineralogy and geochemistry of claystones from the Guadalupian–Lopingian boundary at Penglaitan, South China: Insights into the pre-Lopingian geological events

Yu-Ting Zhong [a,b], Bin He [a,c], Yi-Gang Xu [a,*]

[a] State Key Laboratory of Isotope Geochemistry, Guangzhou Institute of Geochemistry, Chinese Academy of Sciences, Guangzhou 510640, China
[b] University of Chinese Academy of Sciences, Beijing 100039, China
[c] Faculty of Earth Sciences, China University of Geosciences, Wuhan, Hubei 430074, China

ARTICLE INFO

Article history:
Received 12 March 2012
Received in revised form 20 September 2012
Accepted 22 October 2012
Available online 2 November 2012

Keywords:
Claystones
Geochemistry
Mineralogy
Detrital zircons
Emeishan volcanism
Guadalupian–Lopingian (G/L) boundary
Palaeo-Tethys
Penglaitan
Guangxi

ABSTRACT

The Guadalupian–Lopingian (G/L) boundary, at a stratigraphically well-documented outcrop in Penglaitan, Guangxi Autonomous Region, South China, has been approved as the Global Stratotype Section and Point (GSSP). Several volcanic ashes or tuffs occur at this boundary, but their mineralogy and geochemistry are not available yet and no reliable age for this boundary has been obtained. A combined study of mineralogy, geochemistry and geochronology has been carried out in this study on six layers of claystones collected below (Group 1) and above (Group 2) the G/L boundary at the Penglaitan section. Both Group 1 and Group 2 claystones are likely clastic in origin, rather than volcanic ashes as previously thought. Thus the Penglaitan claystones are not suitable for age determination of the G/L boundary. They are significantly different in terms of mineralogy and geochemistry. Specifically, Group 1 claystones are likely derived from a mafic source which is genetically related to the Emeishan large igneous province, therefore providing additional evidence for the synchroneity between the G/L boundary mass extinction and the Emeishan volcanism. Group 2 samples were derived from a felsic source, of which zircons yield an age spectrum peaked at 262 ± 3 Ma, undistinguishable within the uncertainty from the currently accepted G/L boundary age (260.4 ± 0.4 Ma). Nevertheless, Group 2 samples are not related to Emeishan volcanism, because their negative zircon $\varepsilon_{Hf(t)}$ values differ significantly from those of Emeishan magmas and trace element compositions of zircons are indicative of an arc source, rather than a within-plate source. In consideration of paleogeographic reconstruction, we propose that the Group 2 claystones may have been derived from continental arcs during the palaeo-Tethys evolution. This is the first sedimentary evidence for Permian continental arc in the northern margin of palaeo-Tethys.

1. Introduction

The Guadalupian–Lopingian (G/L) boundary was marked by a major mass extinction of various Permian fossils including corals, fusulinaceans, ammonoids and brachiopods (Jin et al., 1994, 1995, 2006; Stanley and Yang, 1994; Shen and Shi, 1996, 2002; Wang and Sugiyama, 2000; Weidlich et al., 2003), which was called as pre-Lopingian crisis at the very beginning (Jin, 1993) and end-Guadalupian (Stanley and Yang, 1994; Isozaki, 2009a) or G/L boundary (Isozaki, 2003; Isozaki et al., 2004) mass extinction. Recent studies show that timing of G/L mass extinction is roughly consistent with the Emeishan large igneous province (ELIP) (e.g., Zhou et al., 2002; He et al., 2007; Wignall et al., 2009a). Moreover, the largest global drop in sea-level or one major regression in Earth history occurred at the G/L boundary (Ross and Ross, 1987, 1994; Chen et al., 1998; Hallam and Wignall, 1999; Haq and Schutter, 2008). Despite their importance (Isozaki, 2009b), the geological events occurring in this critical period have been far less studied, especially when compared with better documented Permian–Triassic boundary events (e.g., Campbell et al., 1992; Renne et al., 1995; Bowring et al., 1998; Jin et al., 2000; Metcalfe et al., 2001; Mundil et al., 2001, 2004; Yin et al., 2001; Kamo et al., 2003, 2006; Shen et al., 2011). This is probably due to the rarity of continuous G/L boundary sections worldwide. The recently established G/L boundary of the Global Stratotype Section and Point (GSSP) at Penglaitan, Laibin, Guangxi (Jin et al., 2006) provides a good opportunity to mitigate this shortcoming. Paleontological, petrographic and sequence-stratigraphic records in this section (Wang and Jin, 2000; Wang et al., 2004; Jin et al., 2006; Shen et al., 2007; Chen et al., 2009; Wignall et al., 2009b; Yang et al., 2009) yielded useful insights into the G/L boundary events. However, absolute isotopic

* Corresponding author. Tel.: +86 20 85290109; fax: +86 20 85290130.
E-mail address: yigangxu@gig.ac.cn (Y.-G. Xu).

1367-9120/$ - see front matter © 2012 Elsevier Ltd. All rights reserved.
http://dx.doi.org/10.1016/j.jseaes.2012.10.028

dating of the G/L boundary is still lacking, which is critical for the GSSP studies and for the temporal link between the G/L boundary extinction and the Emeishan volcanism. There are several volcanic ashes or tuffs at the G/L boundary of this section (Jin et al., 2006; Shen et al., 2007; Wignall et al., 2009b). Isozaki et al. (2004) also pointed out that there is a volcanic ash layer covered South China at the G/L boundary, but its mineralogy and geochemistry are not documented yet. Recently He et al. (2010) suggested that the G/L boundary claystones at Chaotian, SW China, are clastic rocks rather than acidic tuff. This raises a similar question as to the Penglaitan case. In this paper, we have carried out mineralogical, geochemical and geochronological analyses on six layers of claystones from the G/L boundary of the Penglaitan GSSP section. These data are used to define the nature and provenance of the Penglaitan claystones.

2. Geological background and sampling

Permian rocks are extensively exposed along the emerged riverbank of the Hongshui River, 20 km east of Laibin city, Guangxi Autonomous Region (Fig. 1a). The rocks have not suffered any substantial structural disturbance or metamorphism. The Guadalupian Maokou Formation is 302 m in thickness at this section and is divided into five members (Sha et al., 1990; Shen et al., 2007). The upper member, named the Laibin Limestone, is the key stratigraphic unit for the GSSP. The Laibin Limestone is 11 m thick and contains an interbedded chert-dolomitic limestone in the base, a thinner bedded carbonate in the middle, and massive limestone mixed with volcanic ash in the upper part (Wang et al., 2004; Jin et al., 2006). The overlying Lopingian Heshan Formation, about 80 m in thickness, is composed of dark cherty limestone of basinal facies in the lower part and white bioclastic carbonate of sponge reef facies in the upper part (Jin et al., 2006).

Samples presented here include six claystones near the G/L boundary at the Penglaitan section (23°41′43″N, 109°19′16″E) (Fig. 1a). Detailed subdivision of layers is described by Jin et al. (2006). As shown in Fig. 1b, Sample PLT-1 is 0.5–1 cm thick, brown, interbedded clay in the upper part of the Laibin Limestone, which is 60 cm below the G/L boundary. The other five samples (including PLT-2 to PLT-6) were collected from lower part of Lopingian Heshan Formation, which is roughly stratigraphically correlated with Wangpo bed in northern Sichuan. Sample PLT-2 is between Bed 6k and Bed 7a, which is dark-grey and about 2 cm in thickness. Sample PLT-2 is overlain successively by a thick chert-dolomitic limestone (Bed 7a), a 1 cm grey clay layer (PLT-3), another cherty limestone (Bed 7b) and another 4–8 cm grayish-green clay layer (Bed 7c). Samples PLT-4 and PLT-5 are collected from Bed 7c. Sample PLT-6 is collected 1.5 m far away above the G/L boundary.

For the convenience of description, also because of their distinct mineralogy and composition, the samples collected below the G/B boundary are termed as Group 1, and those above the boundary are termed as Group 2.

3. Analytical techniques

3.1. Mineralogical and whole-rock geochemical analyses

Identification of bulk and clay minerals were carried out on unoriented powder mounts by X-ray diffraction (XRD) (BRUKER D8 ADVANGE in German) at the Guangzhou Institute of Geochemistry, Chinese Academy of Sciences (GIGCAS). Qualitative and semi-quantitative characterization of mineralogy is based on peak intensity measurements on X-ray patterns. The diagnostic peak and the corrective intensity factor are indicated for each mineral. Semi-quantitative determination of the main clay species was based on the height of specific reflections, generally measured on ethylene glycol runs. The intensity of the 10 Å peak was taken as a reference, the other intensities were divided by a weight factor and all identified clay species values were summed up to 100%. Corrective factors were determined by long-term empirical experiments at GIGCAS.

All samples were analyzed for major element compositions at GIGCAS using wave-length X-ray fluorescence spectrometry (XRF). A pre-ignition was used to determine the loss on ignition (LOI) prior to major element analyses. Accuracy is within 1% for major elements. These samples were also selected for ICP-MS analysis of whole-rock trace element compositions. Accuracy for trace and rare elements is within 5%. Sample preparation techniques and other details of procedures are described by Li et al. (2002).

3.2. Zircon U–Pb dating, trace element and Hf isotopic analyses

Zircons were separated from four samples (PLT-1, PLT-2, PLT-5 and PLT-6) using conventional heavy liquid and magnetic techniques and purified by hand-picking under a binocular microscope. Zircons were documented with transmitted and reflected light micrographs as well as cathodoluminescence (CL) images to reveal their external and internal structures prior to U–Pb isotopic analyses to observe the erosion degree and select positions for analyses.

Simultaneous measurement of U–Pb isotopes and trace element concentration in the zircons were performed using a Neptune Laser-ablation ICP-MS hosted at the Institute of Geology and Geophysics, Chinese Academy of Sciences (IGGCAS) in Beijing. The instrumental setting and detailed analytical procedure have been described by Wu et al. (2006).

Zircon in situ Hf isotopic analyses were carried out using the Neptune multicollector ICPMS equipped with a Geolas-193 laser-ablation system (LA-MC-ICPMS) at the IGGCAS too. This machine is a double focusing multi-collector ICP-MS and has the capability of high mass resolution measurements in multiple collector modes. Further external adjustment was not applied for the samples because our determined $^{176}Hf/^{177}Hf$ ratios of 0.282303 ± 0.000020 for zircon standards 91500 are in good agreement with the reported values (Wu et al., 2006). More detail experimental conditions and data collection were described by Wu et al. (2006).

4. Analytical results

4.1. XRD results

Mineral compositions from XRD analyses are listed in Table 1. Representative XRD diagrams are shown in Fig. 2. The studied samples are mainly composed of clay minerals (62.3–96.6%) and variable amount of quartz (3.4–37.6%). The Group 1 and Group 2 samples show a contrasting mineralogy. Most of the Group 2 samples (PLT-3 to PLT-6) contain abundant quartz (27.8–37.6%) and one sample (PLT-2) has a low content of quartz (3.4%). They contain minor anatase (0–0.6%), but no calcite. In contrast, the Group 1 sample (PLT-1) contains no quartz but has 4.5% anatase and 11.1% calcite.

4.2. Major elements

Major element compositions are listed in Table 2. High LOI contents (5.4–8.5%) are consistent with a high percentage of clay minerals or calcite in these samples. The whole rock compositions are characterized by high Al_2O_3 (16.3–24.3%), K_2O (5.1–8.1%) and low Na_2O (<0.1–0.25%) contents. SiO_2 content in sample PLT-1 is 44.7%, much lower than in the Group 2 samples (49.4–67.0%).

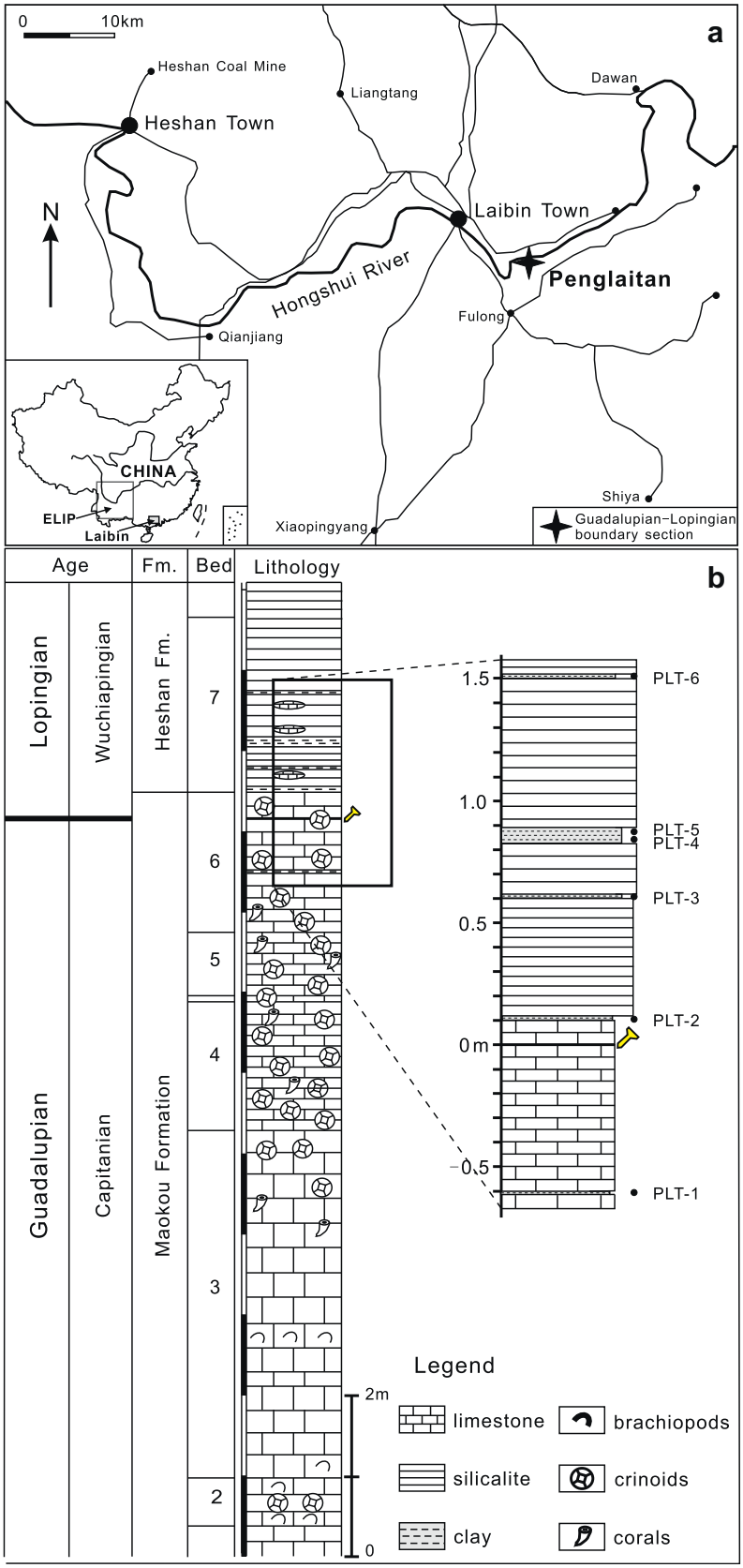

Fig. 1. (a) Location map of Penglaitan section in the Laibin area, South China; and (b) stratigraphy of the Penglaitan section (after Jin et al. (2006)) and sampling localities at the Penglaitan section.

Table 1
Mineral composition from XRD analyses of G–LB claystones at the Penglaitan section.

Sample	Mineral compositions (wt.%)
PLT-1	Illite 19.6; Montmorillonite 29.9; Celadonite 34.7; Calcite 11.1; Anatase 4.5
PLT-2	Illite 39.8; Montmorillonite 14.5; Celadonite 42.3; Quartz 3.4
PLT-3	Illite 25.1; Montmorillonite 12.4; Celadonite 33.4; Quartz 28.5; Anatase 0.6
PLT-4	Illite 27; Montmorillonite 8; Celadonite 27.3; Quartz 37.6
PLT-5	Illite 30; Montmorillonite 6.2; Celadonite 33.4; Quartz 29.8; Anatase 0.6
PLT-6	Kaolinite 4.3; Montmorillonite 8.3; Celadonite 59.6; Quartz 27.8

However, TiO_2 and Fe_2O_3 in PLT-1 (4.9%, 9.1%, respectively) are significantly higher than in the Group 2 samples (0.5–0.9%, 2.1–4.5%, respectively).

Al_2O_3/TiO_2 is a useful indictor for provenance of sedimentary rocks. It is less than 7 for the Group 1 samples, and is greater than 7 for the Group 2 samples. The compositional differences between Group 1 and Group 2 samples is also reflected by much higher contents of TiO_2, Fe_2O_3, CaO and P_2O_5 in Group 1 (PLT-1) than in Group 2 samples (PLT-2 to PLT-6). All these suggest that the nature and composition of claystones below and above the G/L boundary are totally different.

In Fig. 3a, major element compositions of six Penglaitan samples are compared with those of the Post-Archaean Australian Shale composite (PAAS; Taylor and McLennan, 1985), which is regarded as the best representatives of the upper continental crust composition (e.g., Condie, 1993). The Penglaitan samples show composition comparable to PAAS with only slightly higher MgO and K_2O, and slightly lower SiO_2.

4.3. Whole-rock trace elements

Group 1 and Group 2 claystones are also distinct in terms of minor and trace element compositions (Table 2). Total rare earth element (REE) contents in Group 1 sample ($\sum$REE = 241 ppm) are considerably lower than in Group 2 samples ($\sum$REE = 659–1427 ppm). As shown in chondrite-normalized REE patterns (Fig. 3b, normalization values are after Sun and McDonough (1989)), Group 1 sample possesses a very weak negative Eu anomaly ($\delta Eu = 0.83$, $\delta Eu = Eu_{CN}/(Sm_{CN} + Gd_{CN})^{1/2}$, the subscript CN denotes chondrite-normalized), whereas Group 2 samples have strong negative Eu anomalies ($\delta Eu = 0.18–0.47$). Group 1 sample displays less fractionated REE pattern ($(La/Yb)_{CN} = 6.4$) than the Group 2 samples ($(La/Yb)_{CN} = 7.9–15.3$). Fig. 3b compares the REE patterns of the Group 1 and Group 2 sediments with those of Emeishan basalts (Xiao et al., 2004), Emeishan rhyolite (Xu et al., 2010), and Permian arc-related felsic rocks (Li et al., 2006). The compositional similarity between Group 1 (PLT-1) and Emeishan basalts suggests a genetic link between them. On the other hand, the Group 2 samples (PLT-2 to PLT-6) compositionally resemble felsic rocks (Fig. 3b). All six samples have much higher REE contents than PAAS (Fig. 3c). Specifically, Group 2 samples show a strong negative Eu anomaly.

4.4. Zircon U–Pb geochronology

Given few zircon crystals separated from the Group 1 sample (PLT-1), the dating results are not statistically significant. Abundant zircons were separated from three Group 2 samples (PLT-2, PLT-5 and PLT-6) and yield meaningful U–Pb isotopic ages (Table 3). Th/U values in all analyzed zircons >0.1. This, combined

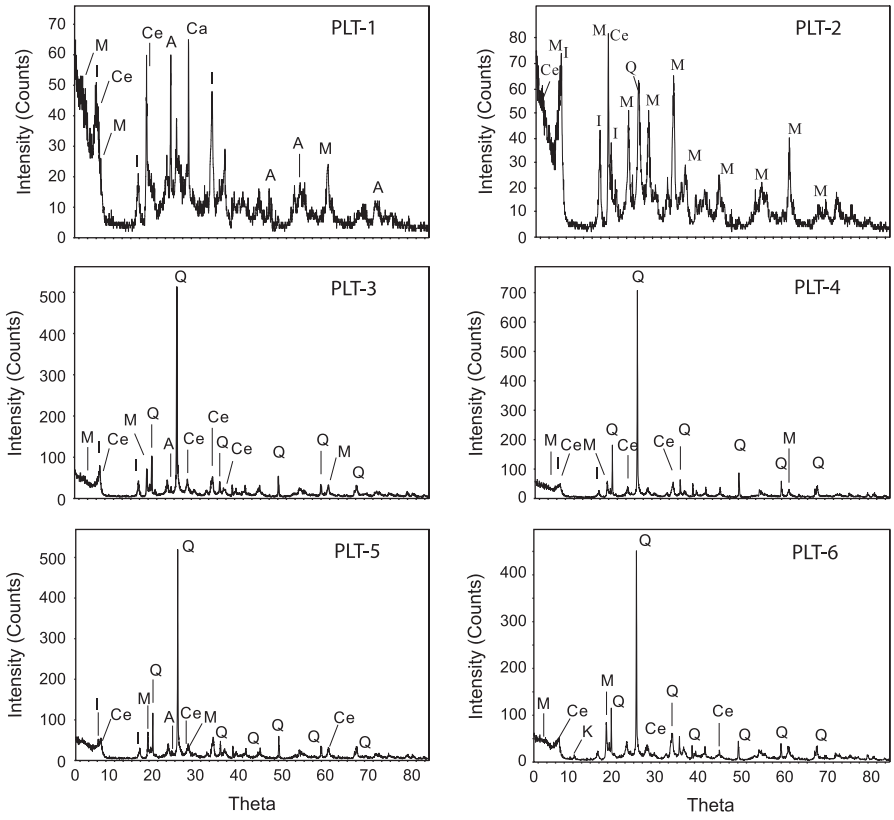

Fig. 2. Representative XRD patterns of G/L boundary claystones at the Penglaitan section. M: Montmorillonite; Ce: celadonite; A: anatase; Q: quartz; P: palygorskite; Ch: chlorite; Ca: calcite; I: illite.

Table 2
Major and trace elements of G–LB claystones at the Penglaitan section.

	PLT-1	PLT-2	PLT-3	PLT-4	PLT-5	PLT-6
Al_2O_3	18.05	24.25	18.33	16.33	17.86	20.08
CaO	3.63	0.52	0.53	0.39	0.56	0.58
Fe_2O_3	9.07	4.54	2.33	2.11	2.45	2.84
K_2O	6.91	8.13	6.46	5.11	6.32	5.53
MgO	3.55	3.93	3.23	2.87	3.25	2.93
MnO	0.03	0.01	0.08	0.00	0.07	0.03
Na_2O	<0.1	<0.1	<0.1	<0.1	<0.1	0.25
P_2O_5	0.68	0.10	0.16	0.04	0.13	0.10
SiO_2	44.69	49.39	62.32	66.96	62.98	61.08
TiO_2	4.93	0.79	0.89	0.49	0.70	0.70
L.O.I	8.45	8.20	5.55	5.59	5.37	5.61
Total	99.98	99.85	99.87	99.90	99.70	99.73
Al_2O_3/TiO_2	3.66	30.68	20.72	33.19	25.61	28.86
Sc	23.12	6.57	9.04	2.99	6.88	5.48
Ti	26046	4212	4688	3088	4357	3310
V	546.7	45.0	76.0	14.4	57.4	33.1
Cr	82.89	34.52	65.91	13.99	36.83	13.4
Mn	299.3	67.1	646.1	31.78	615.0	228.0
Co	42.42	2.40	4.39	0.67	3.34	8.04
Ni	263.70	42.57	96.46	32.88	73.35	34.77
Cu	205.50	28.06	18.24	7.51	19.83	15.54
Zn	200.40	255.40	82.49	218.40	102.10	168.20
Ga	24.75	66.04	42.51	39.67	42.71	45.19
Ge	12.75	3.81	4.03	2.93	3.43	2.86
Rb	193.10	260.70	167.40	169.50	165.50	151.30
Sr	78.48	38.45	58.77	35.14	50.85	28.71
Y	75.86	179.50	130.10	89.02	124.90	103.70
Zr	310.4	2430.8	1107.0	972.2	998.7	1605.8
Nb	47.74	206.50	123.00	148.30	148.70	148.80
Cs	16.55	10.74	8.50	8.39	8.65	10.93
Ba	61.63	55.78	76.76	43.50	71.51	52.37
La	38.79	269.50	176.40	109.30	146.30	227.20
Ce	87.25	598.10	472.70	279.50	355.60	443.20
Pr	12.41	81.02	62.11	39.21	51.64	49.70
Nd	51.91	288.90	218.10	134.80	182.00	181.00
Sm	11.16	49.87	37.50	24.07	31.30	32.60
Eu	3.05	2.74	5.35	2.84	4.23	3.76
Gd	11.12	43.62	30.35	20.38	25.47	26.88
Tb	1.69	6.84	4.65	3.36	3.93	4.15
Dy	9.95	38.36	27.85	19.03	22.66	24.23
Ho	2.02	7.48	5.73	3.60	4.49	4.56
Er	5.77	19.38	16.62	10.05	12.69	10.84
Tm	0.77	2.68	2.32	1.52	1.85	1.62
Yb	4.37	15.96	14.45	9.93	11.75	10.69
Lu	0.61	2.35	2.07	1.50	1.74	1.80
Hf	11.19	59.44	38.29	32.99	33.51	39.47
Ta	3.11	18.55	11.93	9.80	9.85	11.36
Pb	23.01	19.30	5.90	5.38	11.23	10.58
Th	7.78	56.44	34.12	27.99	30.28	34.62
U	6.97	21.22	16.99	9.26	17.70	11.31
∑REE	240.9	1426.8	1076.2	659.1	855.7	1022.2
δEu	0.83	0.18	0.47	0.38	0.44	0.38
$(La/Yb)_{CN}$	6.37	12.11	8.76	7.90	8.93	15.25
$(La/Sm)_{CN}$	2.24	3.49	3.04	2.93	3.02	4.50
$(Gd/Lu)_{CN}$	2.24	2.30	1.81	1.68	1.81	1.85

$\delta Eu = Eu_{CN}/(Sm_{CN} + Gd_{CN})^{1/2}$. CN: Chondrite normalized, normalization value after Sun and McDonough (1989); ∑REE means total rare earth elements.

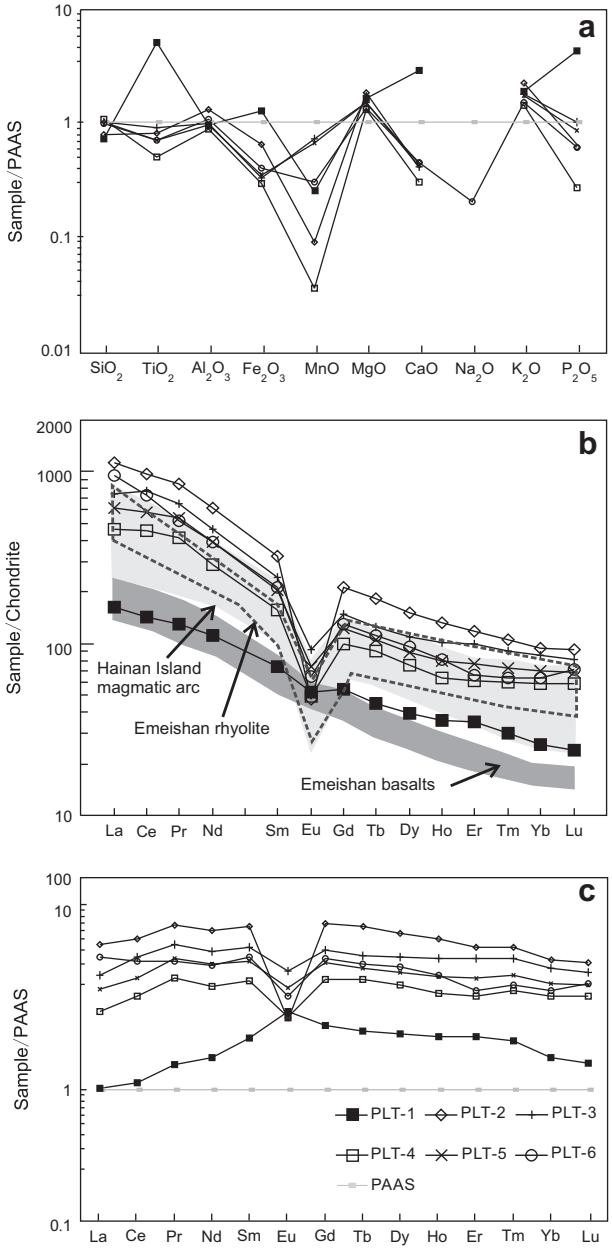

Fig. 3. (a) PAAS-normalized major element diagram, normalization values are after Taylor and McLennan (1985); (b) chondrite-normalized REE patterns diagram, normalization values are after Sun and McDonough (1989); and (c) PAAS-normalized rare earth element diagram for the Penglaitan samples, normalization values are after Taylor and McLennan (1985); Emeishan basalts data are compiled from Xiao et al. (2004); Emeishan rhyolite data are complied from Xu et al. (2010); Hainan Island magmatic arc data are collected from Li et al. (2006).

with zircon morphology and CL images, suggests that all of the detrital zircons have igneous origins.

Sample PLT-2 was collected from the basal part of Heshan Formation, which is interbeded between Bed 6k and Bed 7a (Fig. 1b). Detrital zircons from this sample are clear, pale yellow. Rounded morphology is common, with a few showing subhedral shapes. 93 analyses on these detrital zircons are mostly concordant (Fig. 4a) and yield a wide range from 2509 Ma to 258 Ma, suggesting a complex source. Major age group peaks at 812, 453, and 269 Ma (Fig. 4b).

Sample PLT-5 was collected from uppermost part of Bed 7c at the Penglaitan section (Fig. 1b). Analyses on 108 zircons from this sample are very similar to those of sample PLT-2. Therefore the interpretation is identical. As shown in Fig. 4c, these detrital zircon ages have a wide range from 3274 Ma to 256.5 Ma, with major age group peaks at 822, 439 and 260 Ma (Fig. 4d). One grain yields a significantly old age (3274 Ma).

Similar results (Fig. 4e) are obtained for the sample PLT-6, which was collected 1.5 m above the G/L boundary (Fig. 1b). The ages of 81 zircons from PLT-6 range from 3315 Ma to 258 Ma, with major age peaks at 850 and 266 Ma (Fig. 4f). One grain has a significantly older age (3315.9 Ma) than the other grains.

Table 3
LA-ICP-MS zircon U–Pb data for claystone samples from the Penglaitan section.

Sample/spot	U (ppm)	Th (ppm)	$^{232}Th/^{238}U$	$^{207}Pb/^{206}Pb$	2σ	$^{207}Pb/^{235}U$	2σ	$^{206}Pb/^{238}U$	2σ	$^{206}Pb/^{238}U$	Age
PLT-1											
1	247.77	119.82	0.48	0.11564	0.0049	5.6581	0.22466	0.34387	0.00767	1905.3	±36.81
2	159.75	333.46	2.09	0.07057	0.01184	1.48082	0.23793	0.14747	0.00827	886.8	±46.45
3	279.81	135.58	0.48	0.07165	0.00843	1.49601	0.16811	0.14675	0.006	882.7	±33.72
4	406.87	363.03	0.89	0.07114	0.00437	1.52567	0.08881	0.15072	0.00366	905	±20.51
5	519.82	210.72	0.41	0.11284	0.00422	5.49227	0.19184	0.34211	0.00691	1896.8	±33.21
6	740.2	373.95	0.51	0.04529	0.00753	0.26656	0.04291	0.04136	0.00183	261.3	±11.34
7	359.66	200.72	0.56	0.18592	0.00539	13.92212	0.37263	0.52632	0.01041	2725.9	±43.97
8	321.55	248.22	0.77	0.05437	0.00482	1.05753	0.09066	0.13671	0.00376	826	±21.31
9	760.01	496.74	0.65	0.05719	0.00645	0.3344	0.03607	0.0411	0.00145	259.6	±8.98
10	250.31	201.03	0.80	0.18278	0.00574	13.75744	0.39831	0.529	0.01102	2737.3	±46.44
11	494.63	302.6	0.61	0.06533	0.0071	1.45655	0.15114	0.15668	0.00601	938.3	±33.51
12	243.59	124.2	0.51	0.06892	0.00617	1.50098	0.12791	0.15307	0.00501	918.1	±28.02
13	263.2	241.47	0.92	0.05607	0.00698	0.53175	0.06376	0.06666	0.00243	416	±14.66
14	235.57	274	1.16	0.0693	0.00952	1.44597	0.18904	0.14665	0.00716	882.1	±40.28
15	709.05	311.14	0.44	0.05566	0.00403	0.48778	0.03376	0.06159	0.00146	385.3	±8.85
16	318.86	272.74	0.86	0.05581	0.0046	1.06788	0.08458	0.13446	0.00353	813.2	±20.08
PLT-2											
1	222.28	84.13	0.38	0.15226	0.00243	9.19156	0.13753	0.43791	0.00693	2341.3	±31.06
2	305.92	250.53	0.82	0.1098	0.00151	4.81348	0.06123	0.31801	0.00424	1780	±20.72
3	74.32	64	0.86	0.15965	0.00205	10.39351	0.12636	0.47227	0.00661	2493.5	±28.93
4	234.51	204.07	0.87	0.1589	0.00121	10.36432	0.07635	0.47316	0.00528	2497.4	±23.09
5	77.94	36.57	0.47	0.06853	0.00209	1.35721	0.03831	0.14366	0.00251	865.3	±14.17
6	211.01	123.91	0.59	0.05693	0.00279	0.48826	0.02196	0.06221	0.00148	389.1	±8.98
7	110.51	93.66	0.85	0.06588	0.00187	1.2502	0.03283	0.13767	0.0023	831.5	±13.01
8	183.97	80.51	0.44	0.06761	0.00273	1.27795	0.04721	0.13711	0.0031	828.3	±17.55
9	100.85	57.59	0.57	0.06687	0.00207	1.27239	0.0363	0.13803	0.00246	833.5	±13.92
10	356.37	205.9	0.58	0.0582	0.00108	0.68551	0.0117	0.08545	0.0011	528.6	±6.54
11	154.5	198.9	1.29	0.06826	0.0067	1.31106	0.11815	0.13933	0.00682	840.9	±38.57
12	145.02	91.03	0.63	0.07046	0.0012	1.53428	0.02408	0.15796	0.00206	945.4	±11.47
13	653.43	252.85	0.39	0.05809	0.00095	0.62287	0.00944	0.07779	0.00096	482.9	±5.73
14	266.44	105.99	0.40	0.05427	0.00335	0.30733	0.01736	0.04108	0.00116	259.5	±7.2
15	165.82	76.18	0.46	0.11009	0.00169	4.89032	0.06955	0.32224	0.0045	1800.6	±21.95
16	133.46	133.23	1.00	0.16348	0.00189	10.48055	0.11488	0.46503	0.00612	2461.7	±26.91
17	390.19	83.79	0.21	0.0715	0.00162	1.54079	0.03194	0.15632	0.00238	936.3	±13.29
18	123.5	131.28	1.06	0.17013	0.00186	10.83029	0.11233	0.46176	0.00593	2447.3	±26.13
19	100.97	47.43	0.47	0.06768	0.00577	1.26639	0.09923	0.13571	0.00574	820.4	±32.6
20	218.33	54.16	0.25	0.11581	0.00136	5.44329	0.05983	0.34091	0.00423	1891.1	±20.35
21	453.05	84.3	0.19	0.11667	0.00104	5.44806	0.04584	0.33868	0.00381	1880.3	±18.33
22	377.99	113.62	0.30	0.05465	0.0027	0.30997	0.01407	0.04114	0.00094	259.9	±5.84
23	67.65	16.15	0.24	0.13994	0.00127	7.95111	0.06842	0.41229	0.00475	2225.4	±21.68
24	200.9	82.02	0.41	0.05049	0.00234	0.2873	0.01231	0.04129	0.00088	260.8	±5.45
25	38.77	26.18	0.68	0.10932	0.00154	4.73995	0.06224	0.31463	0.00413	1763.4	±20.26
26	74.71	93.93	1.26	0.10586	0.00111	4.48217	0.04387	0.30722	0.00358	1727	±17.64
27	66.35	43.9	0.66	0.06701	0.00126	1.25092	0.02187	0.13545	0.00176	818.9	±9.98
28	24.26	19.01	0.78	0.10385	0.00248	4.18532	0.09221	0.29243	0.00517	1653.7	±25.8
29	204.14	152.58	0.75	0.16388	0.00167	10.38155	0.10044	0.45966	0.0057	2438.1	±25.15
30	335.08	103.31	0.31	0.05093	0.00253	0.2867	0.01341	0.04085	0.00084	258.1	±5.19
31	161.63	135.79	0.84	0.06593	0.00111	1.21643	0.0191	0.13386	0.00168	809.9	±9.55
32	258.99	213.61	0.82	0.05586	0.0017	0.56927	0.016	0.07394	0.00121	459.9	±7.24
33	255.46	192.36	0.75	0.11235	0.00079	4.81104	0.0323	0.31069	0.00328	1744.1	±16.11
34	59.75	47.57	0.80	0.16513	0.00155	10.83192	0.09727	0.47591	0.00568	2509.4	±24.83
35	938.89	109.32	0.12	0.06786	0.00049	1.29297	0.00882	0.13823	0.00143	834.7	±8.08
36	134.9	118.42	0.88	0.06593	0.00128	1.1905	0.02147	0.131	0.00175	793.6	±9.95
37	153.73	117.38	0.76	0.06622	0.0015	1.22456	0.02582	0.13415	0.00193	811.5	±10.97
38	73.48	50.23	0.68	0.05552	0.00165	0.50431	0.01411	0.06589	0.00097	411.4	±5.85
39	50.64	39.34	0.78	0.06371	0.00289	1.00417	0.04186	0.11434	0.00266	697.9	±15.39
40	26.15	45.33	1.73	0.06076	0.00471	0.7893	0.05932	0.09424	0.00227	580.6	±13.38
41	263.18	79.4	0.30	0.05296	0.00121	0.30099	0.00639	0.04123	0.00056	260.5	±3.44
42	76.36	61.8	0.81	0.11229	0.00127	5.11842	0.05404	0.33067	0.00399	1841.6	±19.34
43	195.76	184.98	0.94	0.11149	0.00117	4.89647	0.04813	0.3174	0.00377	1777	±18.44
44	202.56	239.83	1.18	0.05751	0.00227	0.4606	0.01673	0.05794	0.00113	363.1	±6.9
45	152.44	46.89	0.31	0.05067	0.00389	0.33328	0.02407	0.04763	0.00141	300	±8.69
46	208.74	141.8	0.68	0.05838	0.00227	0.66341	0.02399	0.08239	0.00157	510.3	±9.38
47	440.81	90.95	0.21	0.0733	0.00113	1.73168	0.02467	0.17144	0.00218	1020	±12.01
48	220.51	176.13	0.80	0.05813	0.00256	0.68537	0.02787	0.08565	0.00188	529.8	±11.14
49	168.61	176.12	1.04	0.05956	0.00162	0.70941	0.01779	0.08661	0.00135	535.5	±8.02
50	91.45	61.88	0.68	0.11912	0.00432	5.40728	0.17946	0.33044	0.00894	1840.5	±43.31
51	247.01	39.24	0.16	0.04962	0.00198	0.27892	0.01046	0.04112	0.00072	259.8	±4.46
52	174.64	96.1	0.55	0.08281	0.0021	1.99834	0.04589	0.17669	0.00304	1048.9	±16.64
53	215.98	89.18	0.41	0.07214	0.00171	1.33286	0.02876	0.13542	0.00212	818.7	±12.01
54	189.01	112.71	0.60	0.0562	0.00239	0.57043	0.02252	0.07445	0.00151	462.9	±9.05
55	226.05	110.18	0.49	0.05704	0.00207	0.52208	0.01765	0.06721	0.0012	419.3	±7.26
56	316.45	219.06	0.69	0.05587	0.00127	0.56292	0.01175	0.07411	0.00105	460.9	±6.31

(*continued on next page*)

Table 3 (*continued*)

Sample/spot	U (ppm)	Th (ppm)	$^{232}Th/^{238}U$	$^{207}Pb/^{206}Pb$	2σ	$^{207}Pb/^{235}U$	2σ	$^{206}Pb/^{238}U$	2σ	$^{206}Pb/^{238}U$	Age
57	196.62	132.32	0.67	0.05665	0.00237	0.60316	0.02337	0.07839	0.00159	486.5	±9.52
58	223.16	107.25	0.48	0.05395	0.00228	0.3021	0.01167	0.04141	0.00086	261.6	±5.33
59	292.31	135.1	0.46	0.10687	0.00105	4.06851	0.03699	0.2818	0.00328	1600.4	±16.49
60	148.84	84.62	0.57	0.05662	0.00264	0.34573	0.01481	0.04524	0.00099	285.2	±6.1
61	195.54	140.46	0.72	0.07072	0.00202	1.57797	0.04111	0.16546	0.00301	987	±16.67
62	351.5	207.72	0.59	0.14812	0.00143	8.70146	0.07888	0.43634	0.0053	2334.2	±23.79
63	82.53	91.81	1.11	0.08956	0.00249	3.26192	0.08336	0.27076	0.00524	1544.6	±26.57
64	129.51	217.21	1.68	0.06857	0.00254	1.32677	0.0447	0.14395	0.00309	866.9	±17.41
65	214.58	251.97	1.17	0.05675	0.00114	0.60057	0.01116	0.07677	0.00102	476.8	±6.09
66	253.73	123.89	0.49	0.06916	0.00066	1.33917	0.0121	0.14048	0.00154	847.4	±8.7
67	597.45	322.91	0.54	0.08906	0.00085	2.49713	0.02228	0.2034	0.00228	1193.6	±12.23
68	151.13	74.07	0.49	0.06928	0.00083	1.35135	0.01512	0.1415	0.00162	853.1	±9.16
69	126.68	43.16	0.34	0.06739	0.00144	1.40796	0.0279	0.15155	0.00216	909.6	±12.09
70	730.37	291.55	0.40	0.06822	0.00096	1.32909	0.01722	0.14131	0.00172	852	±9.71
71	547.64	138.25	0.25	0.07103	0.00082	1.45168	0.01549	0.14823	0.00171	891	±9.58
72	117.01	101.91	0.87	0.05691	0.00249	0.38259	0.01556	0.04876	0.00098	306.9	±6
73	419.71	115.51	0.28	0.16356	0.00089	10.72887	0.0585	0.4757	0.00496	2508.5	±21.65
74	107.02	98.34	0.92	0.07762	0.00167	1.88503	0.03709	0.17613	0.00269	1045.8	±14.74
75	188.34	100.12	0.53	0.06512	0.00089	1.21361	0.0154	0.13515	0.00161	817.2	±9.13
76	192.99	49.94	0.26	0.06915	0.00104	1.54953	0.02166	0.16249	0.00204	970.6	±11.31
77	421.06	117.13	0.28	0.06949	0.00068	1.55766	0.01443	0.16255	0.00181	970.9	±10.05
78	114.21	108.1	0.95	0.09576	0.00102	3.61891	0.03629	0.27406	0.00324	1561.4	±16.37
79	379.17	76.33	0.20	0.14106	0.00081	8.03326	0.04596	0.41297	0.00436	2228.5	±19.87
80	192.54	176.4	0.92	0.07131	0.00074	1.57205	0.01532	0.15985	0.00181	955.9	±10.08
81	159.17	106.06	0.67	0.06381	0.00104	1.24904	0.01895	0.14195	0.00178	855.7	±10.07
82	155.79	32.7	0.21	0.06835	0.00118	1.42598	0.02306	0.1513	0.00195	908.2	±10.91
83	450.21	167.13	0.37	0.0573	0.00073	0.68952	0.00825	0.08726	0.00101	539.3	±5.99
84	161.68	94.97	0.59	0.06241	0.00114	1.17535	0.01986	0.13657	0.00184	825.3	±10.44
85	190.69	189.93	1.00	0.06295	0.00116	1.18623	0.02031	0.13665	0.00183	825.7	±10.35
86	286.32	160.87	0.56	0.05241	0.00287	0.33361	0.01683	0.04616	0.00115	290.9	±7.12
87	222.17	118.21	0.53	0.07816	0.00107	2.16045	0.02727	0.20047	0.00254	1177.8	±13.63
88	439.33	210.12	0.48	0.0558	0.00079	0.56342	0.00741	0.07324	0.00087	455.6	±5.24
89	148.85	80.2	0.54	0.07733	0.00191	2.07988	0.04694	0.19507	0.00333	1148.8	±17.97
90	71.43	75.87	1.06	0.14168	0.00174	8.04956	0.09255	0.41212	0.00559	2224.6	±25.53
91	55.83	44.12	0.79	0.10422	0.00177	4.3254	0.06769	0.30106	0.00451	1696.6	±22.37
92	87.09	50.38	0.58	0.11565	0.00124	5.46978	0.05524	0.34308	0.00427	1901.5	±20.47
93	162.41	36.02	0.22	0.05699	0.00127	0.79351	0.01626	0.10101	0.00147	620.3	±8.61
PLT-5											
1	110.68	108.67	0.98	0.06813	0.00157	1.29288	0.02769	0.1375	0.00201	830.5	±11.37
2	668.03	319.87	0.48	0.0616	0.00078	0.61292	0.00721	0.07209	0.00083	448.8	±5.02
3	186.68	209.29	1.12	0.06537	0.00117	1.16904	0.01947	0.12958	0.0017	785.5	±9.67
4	378.52	177.8	0.47	0.11055	0.00109	4.24075	0.03902	0.27797	0.00326	1581.2	±16.47
5	59.56	53.69	0.90	0.05868	0.00267	0.68703	0.0297	0.08484	0.00159	525	±9.47
6	80.53	60.68	0.75	0.06756	0.00172	1.25767	0.02981	0.13491	0.00206	815.8	±11.67
7	128.01	58.55	0.46	0.07	0.00144	1.43515	0.02716	0.14858	0.00215	893	±12.05
8	222.95	99.87	0.45	0.05581	0.00121	0.57132	0.0116	0.0742	0.00098	461.4	±5.9
9	658.03	567.94	0.86	0.0573	0.00108	0.34783	0.00601	0.044	0.00057	277.6	±3.52
10	335.14	44.09	0.13	0.07409	0.00072	1.81323	0.0165	0.17739	0.00199	1052.7	±10.88
11	32.05	13.85	0.43	0.1251	0.00216	6.19324	0.09946	0.35884	0.00547	1976.7	±25.94
12	367.06	301.11	0.82	0.13168	0.00096	6.69758	0.04682	0.36869	0.00406	2023.2	±19.13
13	242.76	47.69	0.20	0.14728	0.00102	8.48196	0.05688	0.41746	0.00458	2248.9	±20.82
14	34.75	18.85	0.54	0.13123	0.0024	5.89014	0.0993	0.32536	0.00509	1815.9	±24.75
15	635.9	615.92	0.97	0.07057	0.00104	1.57731	0.02153	0.16203	0.00205	968.1	±11.36
16	240.79	122.11	0.51	0.05231	0.00172	0.33425	0.01026	0.04633	0.00076	291.9	±4.69
17	121.65	112.24	0.92	0.05545	0.00378	0.38505	0.02429	0.05035	0.00148	316.7	±9.08
18	16.32	19.41	1.19	0.07115	0.00694	1.3167	0.12094	0.13418	0.0054	811.7	±30.71
19	505.44	255.33	0.51	0.05715	0.00074	0.59075	0.00716	0.07495	0.00087	465.9	±5.2
20	75.79	45.46	0.60	0.16315	0.00165	10.71806	0.10385	0.47633	0.00601	2511.2	±26.25
21	44.32	64.89	1.46	0.15801	0.00234	10.18005	0.14215	0.46714	0.00713	2471	±31.31
22	254.61	89.2	0.35	0.0834	0.00096	2.8143	0.03008	0.24469	0.00292	1411	±15.13
23	251.19	144.34	0.57	0.14276	0.00198	8.4562	0.11002	0.4295	0.00622	2303.5	±28.04
24	374.09	50.94	0.14	0.1081	0.00067	4.68066	0.02804	0.31544	0.00331	1767.4	±16.2
25	93.59	46.82	0.50	0.0661	0.00134	1.36751	0.02588	0.15069	0.00206	904.8	±11.52
26	357.39	259.21	0.73	0.11392	0.00091	5.0586	0.03801	0.32338	0.00358	1806.2	±17.45
27	365.7	240.15	0.66	0.06633	0.00086	1.17029	0.014	0.12847	0.00153	779.1	±8.72
28	124.58	89.8	0.72	0.05221	0.00228	0.29117	0.01202	0.0406	0.00074	256.5	±4.56
29	617.8	167.69	0.27	0.0649	0.00159	1.22536	0.02734	0.13742	0.00219	830.1	±12.43
30	586.58	116.24	0.20	0.10344	0.00067	4.33915	0.02713	0.30526	0.00324	1717.3	±16.02
31	114.78	129.5	1.13	0.06535	0.00161	1.23948	0.02811	0.138	0.00216	833.4	±12.21
32	162.21	92.93	0.57	0.05551	0.00161	0.54645	0.01481	0.07157	0.00111	445.6	±6.66
33	85.68	43.89	0.51	0.10037	0.00214	3.91252	0.07667	0.28335	0.00474	1608.2	±23.81
34	165.17	163.32	0.99	0.06991	0.00144	1.52619	0.02874	0.15865	0.00232	949.3	±12.93
35	56.51	39.92	0.71	0.05429	0.00376	0.41482	0.02734	0.05552	0.0014	348.3	±8.56
36	153.82	105.18	0.68	0.05673	0.00155	0.59261	0.01497	0.07588	0.00118	471.5	±7.07
37	317.98	67.52	0.21	0.05095	0.00167	0.28796	0.00872	0.04105	0.00069	259.4	±4.27

Table 3 (*continued*)

Sample/spot	U (ppm)	Th (ppm)	$^{232}Th/^{238}U$	$^{207}Pb/^{206}Pb$	2σ	$^{207}Pb/^{235}U$	2σ	$^{206}Pb/^{238}U$	2σ	$^{206}Pb/^{238}U$	Age
38	259.43	184.98	0.71	0.07495	0.00151	1.91686	0.03523	0.18574	0.00279	1098.2	±15.14
39	144.09	82.73	0.57	0.05207	0.00291	0.30269	0.0157	0.04221	0.00104	266.5	±6.46
40	281.54	82.63	0.29	0.06068	0.00148	0.74757	0.01667	0.08938	0.00137	551.9	±8.11
41	146.59	72.63	0.50	0.06499	0.00121	1.33947	0.02308	0.1495	0.00204	898.2	±11.45
42	136.93	133.03	0.97	0.10893	0.00101	4.94684	0.04342	0.32936	0.00389	1835.3	±18.85
43	371.56	313.8	0.84	0.06991	0.00101	1.53182	0.02051	0.15888	0.00203	950.5	±11.3
44	99.03	96.21	0.97	0.06355	0.00301	1.0725	0.04639	0.12235	0.00311	744.1	±17.85
45	104.97	152.62	1.45	0.15727	0.00172	10.04009	0.10459	0.46276	0.00615	2451.7	±27.12
46	72.98	65.45	0.90	0.06921	0.00195	1.46378	0.03811	0.15328	0.00262	919.3	±14.63
47	67.94	51.24	0.75	0.05596	0.0021	0.54796	0.01915	0.07107	0.00133	442.6	±8.02
48	380.39	107.75	0.28	0.04877	0.00087	0.27802	0.00464	0.04137	0.00052	261.3	±3.23
49	83.59	72.1	0.86	0.06837	0.00165	1.34145	0.02988	0.1424	0.00224	858.2	±12.61
50	177.88	106.23	0.60	0.05399	0.00134	0.30488	0.00701	0.04098	0.0006	258.9	±3.74
51	346.29	188.74	0.55	0.05471	0.00148	0.46295	0.01155	0.06141	0.00097	384.2	±5.9
52	78.71	66.41	0.84	0.15453	0.00346	9.5042	0.19779	0.44632	0.00914	2378.9	±40.74
53	115.27	190.28	1.65	0.06551	0.00096	1.20721	0.01657	0.13372	0.00168	809.1	±9.53
54	96.87	111.41	1.15	0.05539	0.00202	0.45633	0.01562	0.05978	0.00105	374.3	±6.38
55	166.26	95.97	0.58	0.11366	0.00116	5.3109	0.05116	0.33902	0.00415	1882	±19.98
56	97.39	72.44	0.74	0.11026	0.00136	4.85744	0.05575	0.31963	0.00416	1787.9	±20.33
57	216.02	87.59	0.41	0.10855	0.00144	4.68777	0.05778	0.31332	0.0042	1757	±20.61
58	91.19	76.94	0.84	0.13156	0.00221	7.02094	0.10929	0.38719	0.00615	2109.8	±28.57
59	157.35	179.22	1.14	0.06462	0.00121	1.09058	0.01881	0.12244	0.00169	744.6	±9.71
60	299.89	190.94	0.64	0.05435	0.00143	0.53941	0.01309	0.072	0.00113	448.2	±6.77
61	116.28	113.83	0.98	0.06342	0.0016	0.97199	0.02249	0.11119	0.00175	679.7	±10.13
62	75.96	48.73	0.64	0.10692	0.00167	4.73434	0.06847	0.3212	0.00461	1795.6	±22.49
63	251.78	98.02	0.39	0.16702	0.00095	11.13253	0.06386	0.48349	0.00517	2542.5	±22.46
64	46.48	104.78	2.25	0.10822	0.0019	4.9045	0.08009	0.32874	0.00497	1832.2	±24.12
65	69.52	73.67	1.06	0.07181	0.00134	1.57785	0.0273	0.15937	0.0022	953.3	±12.21
66	299.6	36.21	0.12	0.05837	0.00064	0.74996	0.00777	0.0932	0.00105	574.4	±6.19
67	71.66	53.62	0.75	0.10628	0.00158	4.63275	0.06443	0.31617	0.0044	1771	±21.54
68	160.97	88.42	0.55	0.10283	0.0011	4.64099	0.04678	0.32734	0.00396	1825.5	±19.23
69	88.52	87.24	0.99	0.06644	0.00114	1.24443	0.0197	0.13584	0.00177	821.1	±10.04
70	263.93	102.14	0.39	0.06197	0.00088	0.91124	0.01202	0.1067	0.00126	653.6	±7.37
71	279.2	146.01	0.52	0.06617	0.00067	1.19143	0.01142	0.13064	0.00144	791.5	±8.22
72	173.01	175.24	1.01	0.06907	0.00104	1.22415	0.01692	0.12859	0.00159	779.8	±9.11
73	48.12	44.62	0.93	0.12076	0.00201	5.923	0.09169	0.35588	0.00531	1962.6	±25.22
74	252.22	176.38	0.70	0.0512	0.00258	0.29042	0.01353	0.04116	0.00095	260	±5.86
75	246.28	212.72	0.86	0.05729	0.00127	0.52667	0.01075	0.0667	0.00093	416.3	±5.6
76	336.86	201.95	0.60	0.05415	0.00173	0.30589	0.00897	0.04099	0.00068	258.9	±4.24
77	214.38	52.65	0.25	0.18087	0.00145	12.60248	0.0983	0.50557	0.00582	2637.7	±24.91
78	103.6	94.86	0.92	0.07404	0.00162	1.22797	0.02452	0.12034	0.00177	732.5	±10.2
79	244.35	64.64	0.26	0.05993	0.00164	0.53388	0.01349	0.06464	0.00098	403.8	±5.94
80	397.62	119.22	0.30	0.05506	0.00109	0.38158	0.00711	0.05029	0.00063	316.3	±3.86
81	519.4	54.38	0.10	0.07722	0.00067	1.84338	0.01507	0.17323	0.00187	1029.9	±10.28
82	165.49	95.73	0.58	0.1114	0.00085	5.07095	0.03704	0.33032	0.00357	1839.9	±17.32
83	160.17	77.24	0.48	0.05398	0.00315	0.31092	0.01699	0.0418	0.001	264	±6.22
84	222.27	77.06	0.35	0.05496	0.00136	0.4619	0.01075	0.06099	0.00083	381.6	±5.04
85	151.77	66.71	0.44	0.11061	0.00151	4.14345	0.05195	0.27184	0.00354	1550.1	±17.95
86	67.76	82.55	1.22	0.07971	0.00313	2.0014	0.07178	0.18221	0.0043	1079.1	±23.44
87	433.09	174.55	0.40	0.11347	0.00069	5.15561	0.03074	0.32976	0.00341	1837.2	±16.52
88	255.96	154.22	0.60	0.10425	0.0009	4.23514	0.03475	0.29484	0.00325	1665.7	±16.2
89	60.16	26.89	0.45	0.07779	0.0026	2.01072	0.06268	0.18759	0.00357	1108.3	±19.4
90	107.28	46.26	0.43	0.06633	0.00136	1.21723	0.02318	0.13318	0.00184	806	±10.48
91	121.74	71.02	0.58	0.09494	0.00125	2.94917	0.03574	0.22554	0.00281	1311.1	14.76
92	408.19	141.23	0.35	0.05109	0.003	0.30812	0.01672	0.04379	0.00113	276.3	±6.98
93	122.5	103.18	0.84	0.16728	0.00114	10.73658	0.07133	0.46592	0.00504	2465.7	±22.14
94	248.37	90.44	0.36	0.05727	0.00226	0.47154	0.01726	0.05977	0.00114	374.2	±6.91
95	126.21	86.45	0.68	0.07767	0.00083	2.01722	0.0201	0.1885	0.00213	1113.2	±11.57
96	101.52	123.03	1.21	0.06241	0.00156	0.48983	0.01152	0.05696	0.00078	357.1	±4.78
97	136.13	109.02	0.80	0.114	0.00247	5.43364	0.10878	0.3459	0.00612	1915	±29.34
98	460.13	362.55	0.79	0.07303	0.00054	1.73754	0.01237	0.17265	0.00182	1026.7	±10
99	63.14	95.17	1.51	0.06838	0.00117	1.18774	0.01877	0.12601	0.00161	765.1	±9.24
100	90.01	83.1	0.92	0.06556	0.00098	1.31065	0.01825	0.14503	0.00175	873	±9.84
101	78.69	72.84	0.93	0.09688	0.00106	3.63863	0.03716	0.27243	0.00321	1553.1	±16.26
102	150.39	61.3	0.41	0.05374	0.00274	0.30308	0.01419	0.0409	0.00097	258.4	±5.98
103	72.64	34.75	0.48	0.26812	0.00192	24.4739	0.17567	0.662	0.00759	3274.9	±29.44
104	160.51	94.94	0.59	0.06955	0.00225	1.4744	0.04361	0.15374	0.00296	921.9	±16.51
105	351.16	79.11	0.23	0.09683	0.0007	3.72521	0.02565	0.27898	0.00298	1586.2	±15.01
106	360.09	68.33	0.19	0.15602	0.00151	9.47532	0.08732	0.44038	0.00537	2352.4	±24.01
107	580.07	632.5	1.09	0.0531	0.00076	0.29948	0.00398	0.0409	0.00047	258.4	±2.93
108	125.12	69.91	0.56	0.11928	0.00094	5.53712	0.04141	0.33657	0.00371	1870.1	±17.9
PLT-6											
1	74.38	165.02	2.22	0.15957	0.00117	10.28003	0.07163	0.46722	0.00495	2471.3	±21.73
2	485.11	246.12	0.51	0.05269	0.00061	0.29692	0.0032	0.04085	0.00043	258.1	±2.68

(*continued on next page*)

Table 3 (*continued*)

Sample/spot	U (ppm)	Th (ppm)	$^{232}Th/^{238}U$	$^{207}Pb/^{206}Pb$	2σ	$^{207}Pb/^{235}U$	2σ	$^{206}Pb/^{238}U$	2σ	$^{206}Pb/^{238}U$	Age
3	203.04	74.01	0.36	0.06886	0.0006	1.26003	0.01013	0.13264	0.00137	802.9	±7.77
4	184.52	132.56	0.72	0.05076	0.00155	0.29034	0.00815	0.04146	0.00066	261.9	±4.09
5	335.79	116.05	0.35	0.05265	0.00072	0.38678	0.00488	0.05324	0.00059	334.4	±3.63
6	19.81	16.85	0.85	0.15726	0.00274	9.76284	0.16009	0.44988	0.00756	2394.7	±33.6
7	146.43	161.84	1.11	0.0688	0.00093	1.33651	0.01655	0.14075	0.00166	848.9	±9.4
8	104.47	121.88	1.17	0.06231	0.00128	1.01868	0.01918	0.11846	0.00165	721.7	±9.52
9	33.54	21.96	0.65	0.10184	0.00239	4.15917	0.08943	0.29593	0.00538	1671.1	±26.75
10	111.03	56.49	0.51	0.05194	0.0014	0.29418	0.00735	0.04104	0.0006	259.3	±3.74
11	168.9	89.37	0.53	0.05216	0.00094	0.38387	0.00638	0.05333	0.00065	335	±4.01
12	21.46	16.07	0.75	0.06315	0.00228	1.04419	0.03491	0.11985	0.00227	729.7	±13.06
13	110.89	110	0.99	0.06578	0.002	1.21415	0.03352	0.13388	0.00249	810	±14.14
14	55.15	66.73	1.21	0.14985	0.00243	9.91735	0.15243	0.48007	0.00788	2527.6	±34.34
15	86.17	39.58	0.46	0.0495	0.00189	0.28285	0.00995	0.04146	0.00077	261.9	±4.77
16	176.78	118.87	0.67	0.10247	0.00082	4.40471	0.0332	0.31192	0.00344	1750.1	±16.91
17	313.69	313.34	1.00	0.06604	0.0005	1.50313	0.01081	0.16519	0.00175	985.6	±9.68
18	109.7	112.97	1.03	0.05351	0.00204	0.30792	0.01063	0.04178	0.00083	263.8	±5.11
19	265.95	113.86	0.43	0.10338	0.00104	4.27027	0.03987	0.29994	0.00356	1691	±17.64
20	270.5	188.33	0.70	0.10529	0.00103	4.59822	0.04191	0.3172	0.00375	1776	±18.35
21	108.86	129.46	1.19	0.05179	0.00267	0.2922	0.01388	0.04092	0.00097	258.5	±6.01
22	114.14	151.95	1.33	0.10383	0.00084	4.66281	0.03569	0.32571	0.00365	1817.5	±17.73
23	52.22	150.09	2.87	0.11356	0.00175	5.23456	0.07391	0.33431	0.00489	1859.3	±23.64
24	122.18	80.69	0.66	0.07108	0.00206	1.77905	0.0468	0.18152	0.00344	1075.2	±18.77
25	58.87	32.31	0.55	0.05562	0.00147	0.57324	0.01415	0.07475	0.00109	464.7	±6.55
26	92.35	41.19	0.45	0.08129	0.00102	2.34633	0.02716	0.20933	0.00254	1225.2	±13.53
27	170.06	73.61	0.43	0.05625	0.00211	0.70788	0.02422	0.09126	0.00184	563	±10.9
28	20.89	40.95	1.96	0.06665	0.00193	1.25406	0.03375	0.13645	0.00225	824.6	±12.76
29	207.07	102.97	0.50	0.06161	0.00057	1.17669	0.01024	0.1385	0.00151	836.2	±8.53
30	145.61	95.33	0.65	0.09542	0.00098	2.9208	0.02744	0.22199	0.00258	1292.4	±13.59
31	94.62	72.13	0.76	0.05967	0.00074	1.15486	0.01336	0.14035	0.00161	846.6	±9.12
32	124.48	104.21	0.84	0.0593	0.0009	1.14493	0.01602	0.14003	0.00172	844.8	±9.75
33	130.22	118.38	0.91	0.04964	0.00294	0.28665	0.01553	0.04188	0.00114	264.5	±7.06
34	108.99	142.79	1.31	0.05894	0.0025	0.61036	0.0236	0.07511	0.00166	466.9	±9.93
35	393.6	329.76	0.84	0.10814	0.0009	4.80783	0.03779	0.32251	0.00359	1802	±17.47
36	96.66	79.79	0.83	0.18444	0.00111	14.08988	0.08318	0.55416	0.00587	2842.4	±24.35
37	117.85	123.22	1.05	0.10988	0.00095	4.8904	0.03957	0.32286	0.00362	1803.7	±17.62
38	496.79	231.44	0.47	0.10676	0.00072	4.11622	0.02649	0.27971	0.00295	1589.9	±14.84
39	132.44	44.29	0.33	0.05345	0.00349	0.42584	0.02548	0.0578	0.00175	362.2	±10.66
40	42.57	36.65	0.86	0.10802	0.00146	4.56971	0.05704	0.30692	0.004	1725.5	±19.71
41	36.09	13.49	0.37	0.04937	0.007	0.36406	0.04824	0.05351	0.00296	336	±18.12
42	492.44	185.47	0.38	0.16251	0.00083	10.72737	0.0539	0.47898	0.00485	2522.8	±21.13
43	127.46	133.93	1.05	0.15043	0.00146	9.1307	0.08457	0.44056	0.00545	2353.1	±24.39
44	132.44	105.84	0.80	0.10787	0.00169	4.88016	0.07068	0.32837	0.00476	1830.5	±23.08
45	290.71	79.13	0.27	0.06606	0.00127	1.27139	0.02244	0.13967	0.00196	842.8	±11.11
46	81.28	36.35	0.45	0.05616	0.0042	0.35517	0.02485	0.0459	0.00138	289.3	±8.5
47	329.88	201.75	0.61	0.06653	0.00102	1.19619	0.0168	0.13048	0.00165	790.6	±9.43
48	308.57	227.49	0.74	0.27377	0.00195	25.3755	0.18205	0.6726	0.00783	3315.9	±30.19
49	101.23	75	0.74	0.1099	0.00139	4.91194	0.05752	0.32433	0.00421	1810.8	±20.49
50	663.08	373.86	0.56	0.09603	0.00065	3.73286	0.02414	0.28203	0.003	1601.6	±15.07
51	270.97	265.16	0.98	0.05877	0.00133	0.74285	0.01547	0.0917	0.00132	565.6	±7.8
52	389.38	249.64	0.64	0.10641	0.00088	4.83851	0.03809	0.32986	0.00368	1837.7	±17.85
53	155.95	138.54	0.89	0.10723	0.00133	4.84046	0.05565	0.32746	0.00417	1826.1	±20.27
54	64.86	55.09	0.85	0.06863	0.00181	1.35693	0.03288	0.14343	0.00235	864	±13.26
55	89.01	56.04	0.63	0.05175	0.00516	0.29207	0.02699	0.04094	0.00168	258.6	±10.41
56	378.7	170.46	0.45	0.07142	0.00107	1.6257	0.02236	0.16511	0.00209	985.1	±11.58
57	430.23	204.78	0.48	0.06042	0.00069	0.89603	0.00946	0.10756	0.00121	658.6	±7.04
58	163.58	133.85	0.82	0.05653	0.00459	0.32052	0.02368	0.04112	0.00153	259.7	±9.5
59	60.48	45.02	0.74	0.05205	0.00838	0.3229	0.04876	0.04498	0.00272	283.6	±16.79
60	245.17	184.88	0.75	0.06881	0.00111	1.47727	0.02194	0.15566	0.002	932.6	±11.14
61	253.54	130.48	0.51	0.07232	0.00087	1.65125	0.01838	0.16554	0.00192	987.5	±10.63
62	142.15	49	0.34	0.08163	0.00112	2.36102	0.02978	0.2097	0.0026	1227.2	±13.87
63	385.07	72.53	0.19	0.10615	0.00093	4.848	0.04003	0.33108	0.00369	1843.6	±17.86
64	66.76	31.21	0.47	0.13838	0.00303	7.76617	0.15767	0.40684	0.00785	2200.4	±35.99
65	119.7	101.59	0.85	0.1627	0.00108	10.57268	0.06783	0.47127	0.00508	2489.1	±22.26
66	540.33	851.46	1.58	0.07679	0.00057	1.72933	0.01211	0.16332	0.00172	975.2	±9.53
67	261.5	53.3	0.20	0.07385	0.00072	1.70652	0.0154	0.16758	0.00185	998.8	±10.21
68	141.45	68.31	0.48	0.0542	0.00186	0.46221	0.01469	0.06184	0.00107	386.8	±6.49
69	463.82	144.98	0.31	0.06917	0.00045	1.62354	0.0101	0.17022	0.00176	1013.3	±9.67
70	265.06	62.75	0.24	0.10896	0.0009	4.78953	0.03726	0.31879	0.00353	1783.8	±17.25
71	260.59	233.16	0.89	0.13254	0.00117	6.92342	0.05748	0.37884	0.00436	2070.9	±20.39
72	99.74	114.78	1.15	0.07323	0.00108	1.78892	0.02494	0.17718	0.00212	1051.5	±11.62
73	144.59	58.52	0.40	0.06457	0.001	1.15173	0.01643	0.12937	0.00161	784.3	±9.16
74	129.41	61.7	0.48	0.06913	0.0013	1.43241	0.02464	0.15027	0.00207	902.5	±11.59
75	195.96	139.12	0.71	0.05506	0.00122	0.31137	0.00629	0.04101	0.00057	259.1	±3.54
76	443.93	272.27	0.61	0.06705	0.00102	1.29043	0.01809	0.13958	0.00175	842.3	±9.91
77	70.41	51.77	0.74	0.06667	0.0023	1.21632	0.03823	0.13231	0.00264	801.1	±15.01

Table 3 (*continued*)

Sample/spot	U (ppm)	Th (ppm)	$^{232}Th/^{238}U$	$^{207}Pb/^{206}Pb$	2σ	$^{207}Pb/^{235}U$	2σ	$^{206}Pb/^{238}U$	2σ	$^{206}Pb/^{238}U$	Age
78	161.28	94.98	0.59	0.06498	0.00088	1.18305	0.01488	0.13205	0.00157	799.5	±8.95
79	128.36	137.52	1.07	0.05207	0.00188	0.33838	0.01144	0.04713	0.00079	296.9	±4.86
80	706.8	346.84	0.49	0.09304	0.00093	3.00912	0.02772	0.23457	0.00268	1358.4	±14
81	101.25	74.59	0.74	0.10968	0.00094	4.80547	0.03878	0.31777	0.00356	1778.8	±17.4

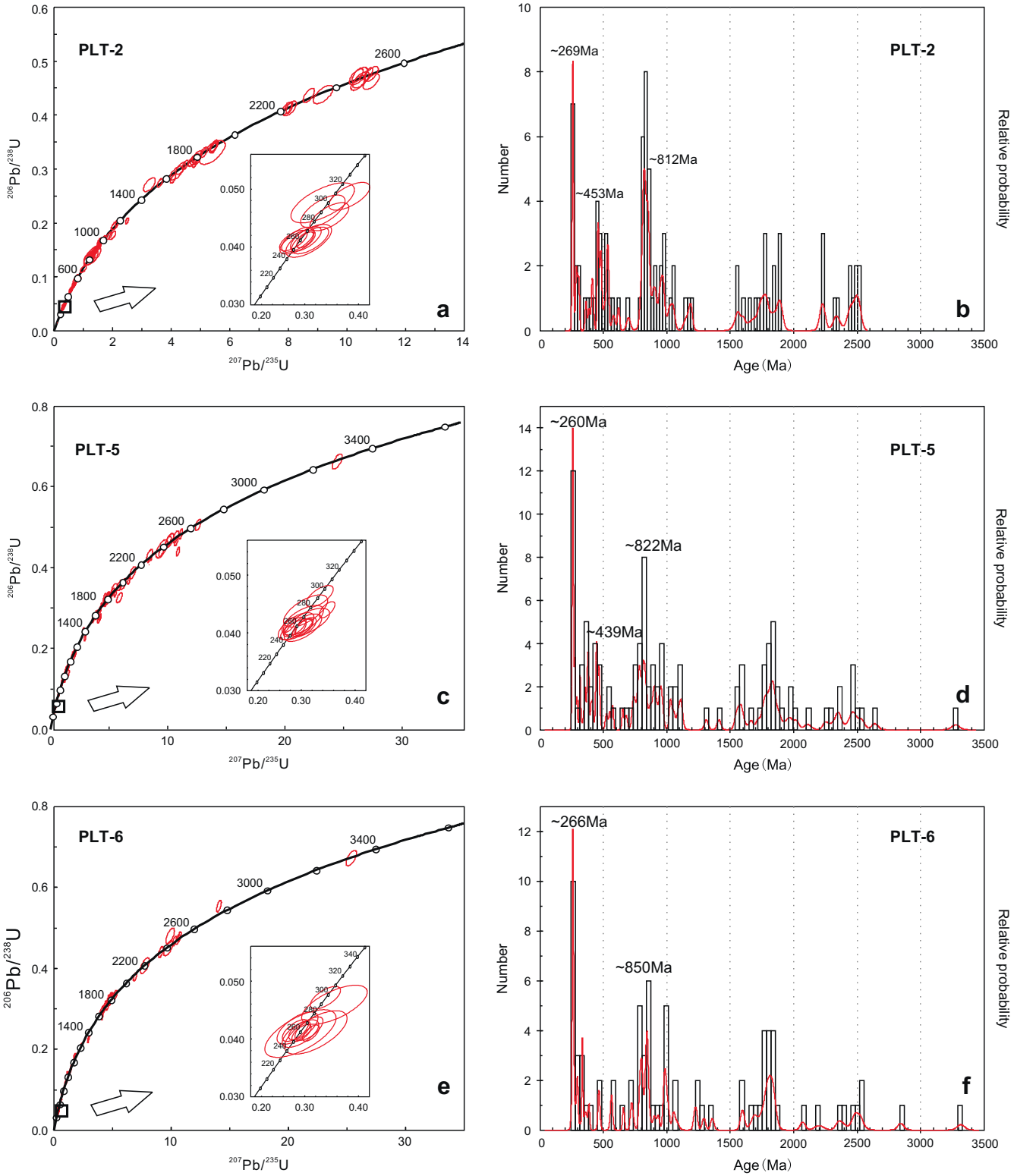

Fig. 4. U–Pb concordia plots of detrital zircons from PLT-2 (a), PLT-5 (c) and PLT-6 (e). Histograms of LA-ICP-MS detrital zircon U–Pb ages for (b) zircons (n = 93) from PLT-2, (d) grains (n = 108) from PLT-5 and (f) zircons (n = 81) from PLT-6.

4.5. Zircon Hf isotopes and trace elements

Hf isotopic compositions were analyzed in the same domain of U–Pb analyses for PLT-2, PLT-5 and PLT-6 (Table 4). Nearly half of the zircons from the analyzed samples have positive or negative $\varepsilon_{Hf(t)}$ values (Fig. 5a), suggesting a derivation from sources with different crystallization history albeit with similar age, namely, mantle or crust. The analyzed zircons with ~260 Ma ages commonly display a flat LREE distribution and a fractionated HREE pattern, with significant positive Ce and negative Eu anomalies (Fig. 5b).

5. Discussions

5.1. Are the Penglaitan G/L boundary claystones acidic tuff?

Intensive research has been carried out on the volcanic ashes from the P–TB. Below are the summarized characteristics of these boundary ashes, which are very useful to determine whether Penglaitan claystones are volcanic acidic ashes or not. (1) A typical acidic tuff or volcanic ash mainly consists of illites and montmorillonites with minor quartzs and feldspars (Zhang et al., 2004,

Table 4
Hf composition for claystone samples from the Penglaitan section.

Sample/spot	Age /Ma	$^{176}Yb/^{177}Hf$	$^{176}Lu/^{177}Hf$	$^{176}Hf/^{177}Hf$	2σ	$\varepsilon_{Hf(0)}$	$\varepsilon_{Hf(t)}$	T_{DM} (Ma)
PLT-2								
1	2341.3	0.009776	0.000408	0.281292	0.000012	−52.3	−0.6	2694
2	1780	0.045942	0.001534	0.281569	0.000014	−42.6	−4.8	2391
3	2493.5	0.011255	0.000371	0.280836	0.000014	−68.5	−13.3	3300
4	2497.4	0.009703	0.000350	0.280858	0.000012	−67.7	−12.4	3269
5	865.3	0.018753	0.000656	0.282556	0.000014	−7.6	11.1	977
6	389.1	0.034031	0.001276	0.282706	0.000014	−2.3	5.9	780
7	831.5	0.046584	0.001739	0.282566	0.000015	−7.3	10.1	991
8	828.3	0.014013	0.000486	0.282237	0.000013	−18.9	−0.9	1413
9	833.5	0.010034	0.000374	0.282458	0.000016	−11.1	7.1	1106
10	528.6	0.016666	0.000611	0.282004	0.000012	−27.2	−15.8	1739
11	840.9	0.023447	0.000962	0.282322	0.000019	−15.9	2.1	1313
12	945.4	0.012629	0.000457	0.281992	0.000015	−27.6	−7.0	1748
13	482.9	0.030492	0.001122	0.282405	0.000013	−13.0	−2.7	1202
14	259.5	0.024625	0.000879	0.282362	0.000015	−14.5	−9.0	1254
15	1800.6	0.017278	0.000629	0.281647	0.000021	−39.8	−0.5	2229
16	2461.7	0.030127	0.001049	0.281131	0.000014	−58.0	−4.7	2959
17	936.3	0.013782	0.000497	0.281724	0.000015	−37.1	−16.7	2117
18	2447.3	0.010618	0.000369	0.281095	0.000013	−59.3	−5.1	2955
19	820.4	0.007796	0.000279	0.282061	0.000013	−25.1	−7.2	1647
20	1891.1	0.015229	0.000529	0.281597	0.000013	−41.6	−0.1	2291
21	1880.3	0.013866	0.000479	0.281595	0.000014	−41.6	−0.3	2291
22	259.9	0.028429	0.001035	0.282900	0.000013	4.5	10.1	500
23	2225.4	0.004040	0.000169	0.281403	0.000015	−48.4	1.1	2530
24	260.8	0.037143	0.001358	0.282251	0.000024	−18.4	−13.0	1427
25	1763.4	0.017361	0.000608	0.281536	0.000013	−43.7	−5.2	2379
26	1727	0.016834	0.000591	0.281561	0.000015	−42.8	−5.1	2343
27	818.9	0.029708	0.001117	0.282336	0.000016	−15.4	2.1	1298
28	1653.7	0.014258	0.000517	0.281493	0.000015	−45.2	−9.1	2431
29	2438.1	0.017953	0.000684	0.281276	0.000014	−52.9	0.6	2735
30	258.1	0.053505	0.001857	0.282312	0.000019	−16.3	−10.9	1359
31	809.9	0.031321	0.001300	0.282515	0.000020	−9.1	8.1	1053
32	459.9	0.044089	0.001520	0.282291	0.000020	−17.0	−7.4	1376
33	1744.1	0.005794	0.000186	0.281636	0.000014	−40.2	−1.6	2218
34	2509.4	0.014194	0.000512	0.281268	0.000015	−53.2	2.2	2734
35	834.7	0.002552	0.000070	0.281833	0.000012	−33.2	−14.9	1947
36	793.6	0.035787	0.001411	0.282540	0.000022	−8.2	8.6	1020
37	811.5	0.029790	0.001229	0.282526	0.000020	−8.7	8.6	1034
38	411.4	0.012805	0.000547	0.282789	0.000015	0.6	9.5	649
39	697.9	0.025992	0.000965	0.282377	0.000014	−14.0	1.0	1236
40	580.6	0.013376	0.000468	0.282188	0.000022	−20.7	−8.1	1481
41	260.5	0.031213	0.001420	0.282867	0.000014	3.4	8.8	552
42	1841.6	0.009837	0.000398	0.281568	0.000013	−42.6	−2.1	2322
43	1777	0.013814	0.000458	0.281506	0.000012	−44.8	−5.8	2409
44	363.1	0.018749	0.000752	0.282010	0.000013	−26.9	−19.2	1737
45	300	0.020511	0.000961	0.282841	0.000018	2.4	8.8	582
46	510.3	0.015876	0.000551	0.282004	0.000016	−27.2	−16.1	1737
47	1020	0.042417	0.001457	0.282127	0.000017	−22.8	−1.2	1605
48	529.8	0.013559	0.000455	0.282168	0.000018	−21.4	−9.9	1508
49	535.5	0.012796	0.000438	0.282155	0.000012	−21.8	−10.2	1525
50	1840.5	0.011080	0.000380	0.281566	0.000012	−42.7	−2.1	2324
51	259.8	0.006259	0.000242	0.282604	0.000012	−6.0	−0.3	901
52	1048.9	0.025631	0.000943	0.281864	0.000020	−32.1	−9.6	1948
53	818.7	0.031343	0.001061	0.282216	0.000018	−19.7	−2.2	1465
54	462.9	0.031806	0.001137	0.282243	0.000023	−18.7	−8.9	1430
55	419.3	0.021442	0.000929	0.282730	0.000021	−1.5	7.5	740
56	460.9	0.030145	0.001202	0.282494	0.000012	−9.8	−0.1	1079
57	486.5	0.029903	0.001102	0.282209	0.000022	−19.9	−9.6	1476
58	261.6	0.008145	0.000339	0.282627	0.000014	−5.1	0.6	871

Table 4 (*continued*)

Sample/spot	Age /Ma	$^{176}Yb/^{177}Hf$	$^{176}Lu/^{177}Hf$	$^{176}Hf/^{177}Hf$	2σ	$\varepsilon_{Hf(0)}$	$\varepsilon_{Hf(t)}$	T_{DM} (Ma)
59	1600.4	0.013182	0.000423	0.281510	0.000015	−44.6	−9.6	2403
60	285.2	0.017263	0.000640	0.282412	0.000013	−12.7	−6.6	1176
61	987	0.015438	0.000592	0.281963	0.000017	−28.6	−7.2	1795
62	2334.2	0.017335	0.000611	0.281119	0.000020	−58.5	−7.2	2942
63	1544.6	0.028245	0.001054	0.281966	0.000018	−28.5	4.8	1812
64	866.9	0.039984	0.001218	0.282268	0.000015	−17.8	0.6	1397
65	476.8	0.043349	0.001451	0.282480	0.000013	−10.3	−0.3	1106
66	847.4	0.014943	0.000512	0.282136	0.000013	−22.5	−4.1	1554
67	1193.6	0.047739	0.001627	0.281800	0.000019	−34.4	−9.3	2073
68	853.1	0.051536	0.001886	0.282540	0.000014	−8.2	9.6	1032
69	909.6	0.012150	0.000429	0.282096	0.000020	−23.9	−4.1	1605
70	852	0.033658	0.001107	0.282269	0.000016	−17.8	0.4	1392
71	891	0.030203	0.001008	0.282119	0.000024	−23.1	−4.0	1597
72	306.9	0.023375	0.001002	0.282524	0.000019	−8.8	−2.2	1031
73	2508.5	0.006986	0.000237	0.281185	0.000013	−56.1	−0.3	2825
74	1045.8	0.032437	0.001284	0.281945	0.000024	−29.3	−7.0	1853
75	817.2	0.013084	0.000448	0.281878	0.000020	−31.6	−13.9	1904
76	970.6	0.005521	0.000204	0.282119	0.000024	−23.1	−1.8	1565
77	970.9	0.004589	0.000134	0.281879	0.000017	−31.6	−10.2	1888
78	1561.4	0.014284	0.000540	0.281394	0.000021	−48.7	−14.6	2566
79	2228.5	0.022453	0.000867	0.281324	0.000017	−51.2	−2.7	2684
80	955.9	0.002048	0.000067	0.282027	0.000013	−26.4	−5.3	1684
81	855.7	0.035507	0.001358	0.282548	0.000018	−7.9	10.2	1007
82	908.2	0.008817	0.000324	0.282079	0.000018	−24.5	−4.7	1624
83	539.3	0.024448	0.000888	0.282385	0.000019	−13.7	−2.1	1223
84	825.3	0.019449	0.000722	0.281994	0.000016	−27.5	−9.7	1758
85	825.7	0.083225	0.003061	0.282651	0.000023	−4.3	12.3	901
86	290.9	0.034922	0.001200	0.282544	0.000021	−8.0	−1.9	1007
87	1177.8	0.016406	0.000583	0.281686	0.000019	−38.4	−12.8	2172
88	455.6	0.032817	0.001210	0.282687	0.000019	−3.0	6.6	806
89	1148.8	0.023903	0.000851	0.282148	0.000018	−22.1	2.7	1551
90	2224.6	0.022156	0.000738	0.280986	0.000016	−63.2	−14.6	3130
91	1696.6	0.019141	0.000642	0.281577	0.000015	−42.2	−5.3	2324
92	1901.5	0.008539	0.000297	0.281420	0.000014	−47.8	−5.8	2516
93	620.3	0.016483	0.000565	0.282514	0.000013	−9.1	4.3	1033
PLT-5								
1	830.5	0.018402	0.000607	0.281939	0.000023	−29.5	−11.5	1829
2	448.8	0.021580	0.000750	0.282389	0.000017	−13.5	−3.9	1212
3	785.5	0.032799	0.001049	0.281996	0.000018	−27.4	−10.7	1771
4	1581.2	0.019465	0.000691	0.281723	0.000031	−37.1	−2.7	2128
5	525	0.023290	0.000805	0.282562	0.000019	−7.4	3.8	973
6	815.8	0.023056	0.000845	0.282383	0.000021	−13.8	3.8	1224
7	893	0.017393	0.000598	0.282391	0.000022	−13.5	5.9	1205
8	461.4	0.018832	0.000679	0.282421	0.000021	−12.4	−2.5	1166
9	277.6	0.050349	0.002124	0.282814	0.000026	1.5	7.2	641
10	1052.7	0.066701	0.002306	0.282288	0.000017	−17.1	4.6	1410
11	1976.7	0.008971	0.000329	0.281648	0.000022	−39.8	3.9	2211
12	2023.2	0.011827	0.000471	0.281320	0.000018	−51.3	−6.9	2661
13	2248.9	0.010320	0.000390	0.281215	0.000018	−55.0	−5.4	2796
14	1815.9	0.012520	0.000442	0.281577	0.000023	−42.3	−2.4	2313
15	968.1	0.030588	0.001068	0.282134	0.000020	−22.6	−1.9	1579
16	291.9	0.027628	0.001063	0.282688	0.000019	−3.0	3.2	801
17	316.7	0.040272	0.001344	0.282438	0.000025	−11.8	−5.1	1162
18	811.7	0.010974	0.000410	0.282111	0.000022	−23.4	−5.7	1584
19	465.9	0.026208	0.001037	0.282285	0.000019	−17.2	−7.3	1367
20	2511.2	0.023988	0.000899	0.281308	0.000022	−51.8	3.0	2707
21	2471	0.017399	0.000593	0.280969	0.000021	−63.8	−9.4	3141
22	1411	0.012261	0.000449	0.282068	0.000020	−24.9	6.0	1645
23	2303.5	0.017185	0.000601	0.281207	0.000022	−55.3	−4.8	2822
24	1767.4	0.015756	0.000522	0.281475	0.000015	−45.9	−7.2	2456
25	904.8	0.015849	0.000547	0.282278	0.000017	−17.5	2.2	1359
26	1806.2	0.013841	0.000591	0.281563	0.000020	−42.8	−3.3	2341
27	779.1	0.045715	0.001486	0.282415	0.000014	−12.6	3.8	1199
28	256.5	0.028502	0.000959	0.282711	0.000024	−2.1	3.3	766
29	830.1	0.004576	0.000200	0.281878	0.000019	−31.6	−13.4	1893
30	1717.3	0.028441	0.001052	0.281644	0.000022	−39.9	−2.9	2258
31	833.4	0.066115	0.002539	0.282569	0.000022	−7.2	9.8	1009
32	445.6	0.021211	0.000759	0.282338	0.000022	−15.4	−5.8	1284
33	1608.2	0.016884	0.000629	0.281937	0.000024	−29.5	5.6	1832
34	949.3	0.020877	0.000700	0.282101	0.000019	−23.7	−3.2	1610
35	348.3	0.018468	0.000756	0.282882	0.000022	3.9	11.4	521
36	471.5	0.025483	0.000916	0.282436	0.000023	−11.9	−1.8	1152
37	259.4	0.049183	0.001712	0.282300	0.000019	−16.7	−11.3	1371
38	1098.2	0.018162	0.000616	0.281666	0.000021	−39.1	−15.3	2202

(*continued on next page*)

Table 4 (*continued*)

Sample/spot	Age /Ma	$^{176}Yb/^{177}Hf$	$^{176}Lu/^{177}Hf$	$^{176}Hf/^{177}Hf$	2σ	$\varepsilon_{Hf(0)}$	$\varepsilon_{Hf(t)}$	T_{DM} (Ma)
39	266.5	0.012960	0.000531	0.282662	0.000017	−3.9	1.9	827
40	551.9	0.017934	0.000629	0.282212	0.000020	−19.8	−7.9	1454
41	898.2	0.020162	0.000722	0.282308	0.000022	−16.4	3.0	1324
42	1835.3	0.016736	0.000578	0.281416	0.000019	−47.9	−7.8	2539
43	950.5	0.030169	0.001025	0.282083	0.000019	−24.3	−4.0	1648
44	744.1	0.055099	0.002020	0.282528	0.000023	−8.6	6.8	1054
45	2451.7	0.029565	0.001039	0.281302	0.000026	−52.0	1.2	2726
46	919.3	0.057140	0.002203	0.282576	0.000026	−6.9	12.1	989
47	442.6	0.017958	0.000689	0.282802	0.000014	1.1	10.6	634
48	261.3	0.043771	0.001529	0.282366	0.000014	−14.4	−8.9	1271
49	858.2	0.054595	0.001992	0.282553	0.000017	−7.8	10.1	1017
50	258.9	0.037952	0.001539	0.282784	0.000016	0.4	5.9	673
51	384.2	0.014086	0.000511	0.282455	0.000014	−11.2	−2.9	1113
52	2378.9	0.019108	0.000664	0.281208	0.000015	−55.3	−3.1	2826
53	809.1	0.060802	0.002180	0.282403	0.000017	−13.0	3.6	1239
54	374.3	0.019458	0.000702	0.282852	0.000016	2.8	10.9	563
55	1882	0.021075	0.000730	0.281517	0.000014	−44.4	−3.4	2412
56	1787.9	0.018069	0.000626	0.281605	0.000014	−41.3	−2.2	2286
57	1757	0.001209	0.000034	0.281590	0.000012	−41.8	−2.8	2272
58	2109.8	0.020338	0.000750	0.281400	0.000016	−48.5	−2.5	2571
59	744.6	0.040491	0.001502	0.282082	0.000015	−24.4	−8.7	1671
60	448.2	0.024337	0.000956	0.282591	0.000015	−6.4	3.2	935
61	679.7	0.036703	0.001354	0.282060	0.000016	−25.2	−10.8	1695
62	1795.6	0.026457	0.000906	0.281453	0.000013	−46.6	−7.8	2510
63	2542.5	0.006926	0.000236	0.280895	0.000013	−66.4	−9.8	3211
64	1832.2	0.011057	0.000380	0.281502	0.000019	−44.9	−4.6	2410
65	953.3	0.036844	0.001369	0.282513	0.000016	−9.2	11.1	1057
66	574.4	0.003381	0.000126	0.282381	0.000010	−13.8	−1.2	1203
67	1771	0.005032	0.000169	0.281567	0.000020	−42.6	−3.4	2310
68	1825.5	0.021205	0.000797	0.281865	0.000023	−32.1	7.6	1940
69	821.1	0.038403	0.001403	0.282029	0.000013	−26.3	−9.0	1742
70	653.6	0.033214	0.001128	0.282410	0.000014	−12.8	1.1	1194
71	791.5	0.013780	0.000474	0.281945	0.000012	−29.2	−12.0	1814
72	779.8	0.060702	0.002213	0.282543	0.000013	−8.1	8.0	1038
73	1962.6	0.016108	0.000547	0.281375	0.000021	−49.4	−6.4	2592
74	260	0.018368	0.000667	0.282656	0.000021	−4.1	1.5	837
75	416.3	0.044180	0.001631	0.282494	0.000014	−9.8	−1.1	1092
76	258.9	0.030533	0.001248	0.282888	0.000013	4.1	9.6	519
77	2637.7	0.045055	0.001656	0.281152	0.000012	−57.3	−1.0	2977
78	732.5	0.016289	0.000574	0.282242	0.000013	−18.7	−2.9	1410
79	403.8	0.044569	0.001551	0.282359	0.000018	−14.6	−6.1	1281
80	316.3	0.033325	0.001199	0.282267	0.000019	−17.9	−11.2	1398
81	1029.9	0.029090	0.000974	0.282096	0.000016	−23.9	−1.8	1628
82	1839.9	0.008900	0.000299	0.281627	0.000013	−40.5	0.1	2237
83	264	0.026142	0.000940	0.282501	0.000019	−9.6	−3.9	1061
84	381.6	0.021204	0.000754	0.282341	0.000017	−15.3	−7.1	1280
85	1550.1	0.029324	0.001056	0.281836	0.000017	−33.1	0.2	1993
86	1079.1	0.012439	0.000427	0.281794	0.000013	−34.6	−11.0	2017
87	1837.2	0.007325	0.000256	0.281540	0.000012	−43.6	−3.0	2351
88	1665.7	0.032204	0.001250	0.282039	0.000019	−25.9	9.7	1721
89	1108.3	0.013147	0.000469	0.282264	0.000025	−18.0	6.2	1376
90	806	0.016707	0.000585	0.282339	0.000015	−15.3	2.2	1276
91	1311.1	0.022322	0.000810	0.281864	0.000016	−32.1	−3.8	1941
92	276.3	0.038263	0.001399	0.282312	0.000024	−16.3	−10.5	1343
93	2465.7	0.020634	0.000696	0.281219	0.000015	−54.9	−0.8	2813
94	374.2	0.031456	0.001118	0.282128	0.000022	−22.8	−14.8	1590
95	1113.2	0.027313	0.000985	0.282094	0.000013	−24.0	−0.1	1632
96	357.1	0.026222	0.000920	0.282877	0.000014	3.7	11.4	530
97	1915	0.015870	0.000542	0.281355	0.000014	−50.1	−8.1	2618
98	1026.7	0.024568	0.000829	0.282003	0.000012	−27.2	−5.1	1751
99	765.1	0.051571	0.001974	0.282616	0.000016	−5.5	10.4	926
100	873	0.018065	0.000663	0.282255	0.000013	−18.3	0.6	1396
101	1553.1	0.023015	0.000873	0.281922	0.000016	−30.1	3.6	1864
102	258.4	0.026537	0.001027	0.282501	0.000014	−9.6	−4.1	1064
103	3274.9	0.014809	0.000528	0.280542	0.000015	−78.8	−6.1	3703
104	921.9	0.027442	0.000952	0.282178	0.000022	−21.0	−1.2	1513
105	1586.2	0.018907	0.000644	0.281567	0.000018	−42.6	−8.1	2338
106	2352.4	0.012185	0.000422	0.280786	0.000016	−70.2	−18.3	3370
107	258.4	0.036182	0.001414	0.282729	0.000014	−1.5	3.9	750
108	1870.1	0.005313	0.000185	0.281385	0.000015	−49.1	−7.6	2555
PLT-6								
1	2471.3	0.022120	0.000796	0.281269	0.000017	−53.2	0.9	2753
2	258.1	0.024095	0.000845	0.282567	0.000016	−7.3	−1.7	967
3	802.9	0.008131	0.000301	0.282109	0.000016	−23.5	−5.9	1583
4	261.9	0.025960	0.000974	0.282574	0.000020	−7.0	−1.4	959

Table 4 (*continued*)

Sample/spot	Age /Ma	$^{176}Yb/^{177}Hf$	$^{176}Lu/^{177}Hf$	$^{176}Hf/^{177}Hf$	2σ	$\varepsilon_{Hf(0)}$	$\varepsilon_{Hf(t)}$	T_{DM} (Ma)
5	334.4	0.031199	0.001118	0.282328	0.000015	−15.7	−8.6	1310
6	2394.7	0.005838	0.000219	0.281288	0.000015	−52.5	0.8	2687
7	848.9	0.014827	0.000512	0.282039	0.000013	−25.9	−7.5	1687
8	721.7	0.065826	0.002334	0.282621	0.000018	−5.3	9.5	927
9	1671.1	0.010344	0.000397	0.281454	0.000015	−46.6	−9.9	2476
10	259.3	0.018034	0.000653	0.282194	0.000017	−20.5	−14.9	1480
11	335	0.016708	0.000741	0.282697	0.000018	−2.7	4.5	782
12	729.7	0.012192	0.000455	0.282543	0.000016	−8.1	7.8	990
13	810	0.007862	0.000309	0.281940	0.000020	−29.4	−11.7	1812
14	2527.6	0.021019	0.000719	0.280866	0.000018	−67.4	−12.0	3290
15	261.9	0.015181	0.000556	0.282678	0.000017	−3.3	2.3	805
16	1750.1	0.005153	0.000248	0.281462	0.000017	−46.3	−7.7	2456
17	985.6	0.027562	0.001004	0.282194	0.000018	−20.4	0.7	1494
18	263.8	0.025580	0.000968	0.282246	0.000016	−18.6	−13.0	1419
19	1691	0.002060	0.000061	0.281594	0.000015	−41.7	−4.1	2267
20	1776	0.010283	0.000374	0.281272	0.000016	−53.0	−14.0	2718
21	258.5	0.019055	0.000697	0.282353	0.000017	−14.8	−9.3	1260
22	1817.5	0.015717	0.000525	0.281420	0.000015	−47.8	−8.0	2530
23	1859.3	0.015092	0.000535	0.281322	0.000015	−51.3	−10.5	2662
24	1075.2	0.029362	0.001032	0.282168	0.000016	−21.4	1.7	1531
25	464.7	0.007395	0.000302	0.282760	0.000016	−0.4	9.7	685
26	1225.2	0.016362	0.000575	0.281996	0.000028	−27.4	−0.8	1748
27	563	0.022182	0.000799	0.282410	0.000022	−12.8	−0.7	1185
28	824.6	0.049352	0.001859	0.282639	0.000022	−4.7	12.5	889
29	836.2	0.017092	0.000589	0.282251	0.000016	−18.4	−0.3	1398
30	1292.4	0.017083	0.000637	0.282272	0.000024	−17.7	10.4	1371
31	846.6	0.021292	0.000736	0.281981	0.000019	−28.0	−9.7	1777
32	844.8	0.007596	0.000279	0.281983	0.000016	−27.9	−9.4	1754
33	264.5	0.023414	0.000931	0.282608	0.000017	−5.8	−0.2	911
34	466.9	0.034705	0.001321	0.282791	0.000019	0.7	10.6	659
35	1802	0.016271	0.000577	0.281437	0.000016	−47.2	−7.8	2510
36	2842.4	0.032227	0.001149	0.281016	0.000016	−62.1	−0.4	3123
37	1803.7	0.020621	0.000711	0.281438	0.000015	−47.2	−7.9	2518
38	1589.9	0.030320	0.001009	0.281560	0.000014	−42.9	−8.6	2370
39	362.2	0.012672	0.000554	0.282455	0.000015	−11.2	−3.4	1115
40	1725.5	0.013839	0.000492	0.281424	0.000015	−47.7	−9.9	2523
41	336	0.033637	0.001465	0.282890	0.000020	4.2	11.2	521
42	2522.8	0.018910	0.000689	0.280974	0.000014	−63.6	−8.2	3142
43	2353.1	0.015884	0.000584	0.281105	0.000016	−58.9	−7.2	2958
44	1830.5	0.007470	0.000264	0.281346	0.000015	−50.4	−10.0	2612
45	842.8	0.014510	0.000530	0.282164	0.000015	−21.5	−3.2	1515
46	289.3	0.015726	0.000594	0.282719	0.000017	−1.9	4.4	748
47	790.6	0.057279	0.001843	0.282365	0.000017	−14.4	2.1	1282
48	3315.9	0.024786	0.000952	0.280646	0.000019	−75.2	−2.5	3605
49	1810.8	0.008023	0.000298	0.281581	0.000013	−42.1	−2.2	2299
50	1601.6	0.040913	0.001538	0.282027	0.000016	−26.4	7.6	1751
51	565.6	0.013142	0.000444	0.282167	0.000018	−21.4	−9.1	1509
52	1837.7	0.011825	0.000474	0.281389	0.000021	−48.9	−8.6	2568
53	1826.1	0.007191	0.000242	0.281371	0.000019	−49.5	−9.2	2577
54	864	0.018961	0.000725	0.282524	0.000015	−8.8	9.9	1024
55	258.6	0.019082	0.000777	0.282853	0.000026	2.8	8.4	563
56	985.1	0.032586	0.001193	0.282129	0.000017	−22.7	−1.8	1592
57	658.6	0.012313	0.000443	0.282339	0.000016	−15.3	−1.0	1272
58	259.7	0.054585	0.001758	0.282714	0.000029	−2.0	3.4	778
59	283.6	0.041904	0.001466	0.282714	0.000020	−2.0	3.9	772
60	932.6	0.010826	0.000387	0.282146	0.000012	−22.1	−1.8	1535
61	987.5	0.013247	0.000461	0.282190	0.000017	−20.6	0.9	1477
62	1227.2	0.016404	0.000552	0.281964	0.000016	−28.6	−1.8	1792
63	1843.6	0.026359	0.000907	0.281532	0.000022	−43.9	−3.9	2402
64	2200.4	0.009403	0.000374	0.281273	0.000022	−53.0	−4.4	2718
65	2489.1	0.017203	0.000653	0.281110	0.000017	−58.8	−4.1	2956
66	975.2	0.038027	0.001260	0.282073	0.000025	−24.7	−4.0	1673
67	998.8	0.019605	0.000706	0.281523	0.000020	−44.2	−22.6	2402
68	386.8	0.028452	0.001015	0.282351	0.000021	−14.9	−6.6	1274
69	1013.3	0.008166	0.000279	0.281658	0.000014	−39.4	−17.2	2194
70	1783.8	0.022927	0.000831	0.281609	0.000021	−41.1	−2.4	2292
71	2070.9	0.024172	0.000818	0.281326	0.000020	−51.1	−6.1	2676
72	1051.5	0.007195	0.000284	0.281441	0.000020	−47.1	−24.1	2486
73	784.3	0.027960	0.001005	0.282335	0.000015	−15.5	1.3	1296
74	902.5	0.028675	0.000961	0.282349	0.000025	−14.9	4.4	1275
75	259.1	0.041879	0.001583	0.282724	0.000026	−1.7	3.7	761
76	842.3	0.019801	0.000685	0.282065	0.000022	−25.0	−6.8	1659

(*continued on next page*)

Table 4 (*continued*)

Sample/spot	Age /Ma	$^{176}Yb/^{177}Hf$	$^{176}Lu/^{177}Hf$	$^{176}Hf/^{177}Hf$	2σ	$\varepsilon_{Hf(0)}$	$\varepsilon_{Hf(t)}$	T_{DM} (Ma)
77	801.1	0.017918	0.000610	0.282050	0.000017	−25.5	−8.2	1676
78	799.5	0.011219	0.000402	0.281940	0.000022	−29.4	−12.0	1818
79	296.9	0.012676	0.000610	0.282611	0.000022	−5.7	0.7	899
80	1358.4	0.024909	0.000959	0.281766	0.000023	−35.6	−6.3	2084
81	1778.8	0.020924	0.000733	0.281637	0.000014	−40.1	−1.4	2249

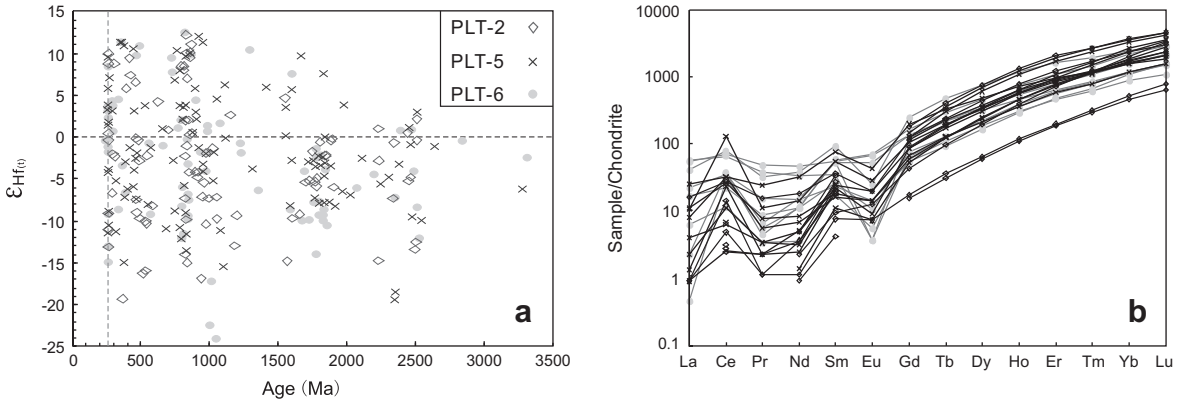

Fig. 5. (a) Plots of $\varepsilon_{Hf(t)}$ values *versus* concordant ages of the zircons from Penglaitan samples; and (b) chondrite-normalized trace element abundances in zircons from PLT-2, PLT-5 and PLT-6 (~260 Ma portion), normalization values are after Sun and McDonough (1989).

2006a,b; Table 6). (2) Acidic tuff, or its altered rocks (i.e., tonsteins) commonly have high Al_2O_3/TiO_2 (Spears and Kanaris-Sotiriou, 1979; Zhou et al., 1982; Zhou and Kyte, 1988). For instance, Al_2O_3/TiO_2 ratio of acidic tuff at Permian–Triassic boundary of Meishan (the GSSP of P–T boundary), and other two sections (Shangsi and Liangfengya) in South China range from 34.5 to 76.9 with an average of 47.6 (Zhou and Kyte, 1988). Moreover, acidic tuffs commonly have strong negative Eu anomalies (Kramer et al., 2001), with Eu/Eu* less than 1 (e.g., 0.23–0.47 in the case of P–TB tuffs, Zhou and Kyte, 1988). (3) Zircons in acidic tuffs at a given boundary, irrespective of their geographic location, generally yield uniform ages (i.e., Mundil et al., 2004; Shen et al., 2011) because they are formed at the same time and are widely distributed over a large-scale area. It has been shown that 2–5 light-colored clay layers steadily occur at the P–TB in the sections spatially separated (Zhou and Kyte, 1988). These P–TB tuffs are indeed well correlated in South China.

Group 1 sample (PLT-1) from Penglaitan consists of 34.7% celadonite, 29.9% montmorillonite, 19.6% illite and a subordinate amount of anatase (4.5%), but contains no quartz and feldspar (Table 1). The contents of Fe_2O_3 and TiO_2 in this sample are significantly higher than in typical acidic tuff. Al_2O_3/TiO_2 of Group 1 sediments is 3.66, similar to that of mafic magmas from the ELIP (2.68–3.61; Xiao et al., 2004), but much lower than that of acidic tuffs (34.5–76.9; Zhou and Kyte, 1988). Group 1 sample displays a very weak negative Eu anomaly (δEu = 0.83), significantly different from acidic tuff which commonly shows strong negative Eu anomaly. The mineralogical and geochemical characteristics therefore suggest that the Group 1 sediments are not acidic tuff. This is further supported by the scattered age distribution of the Group 1 zircons (Table 3), which is consistent with a detrital origin.

The Group 2 claystones contain clay minerals and quartz, but no feldspar. Celadonite accounts for a large proportion (27.3–59.6%) in clay minerals, with a maximum of 59.6% in the sample PLT-6. Very low contents of illite and montmorillonite in Group 2 samples (Table 1) render them different from acidic tuffs or ashes. Quartz content (27.8–37.6%) in four Group 2 samples (PLT-3 to PLT-6) is significantly higher than that of typical acidic tuff. The round shape of most zircons from the Penglaitan samples is also inconsistent with the origin of acidic tuffs. Al_2O_3/TiO_2 of Group 2 samples ranges from 20.7 to 33.2, lower than the values (34.5–76.9) of typical P–T boundary tuffs (Zhou and Kyte, 1988).

The important constraints on the origin of the Penglaitan claystones also come from zircon U–Pb dating, which show a wide age variation ranging from Paleoproterozoic to Permian(Table 3 and Fig. 4). This is in contradiction with a volcanic origin of the G/L boundary claystones. Moreover, the distribution of G/L boundary claystones seems to be laterally discontinuous. A notable example is the lack of G/L boundary claystones in the Tieqiao section, which is only 10 km west of the Penglaitan section. In contrast, the P–TB clay layers, widespread in South China (500–1500 km), are of volcanic origin (Zhou and Kyte, 1988; Yin et al., 1989). The arguments presented above collectively suggest that the Penglaitan Group 2 samples are not air-fall acidic tuff. Instead they are most likely detrital or clastic sedimentary rocks. Similar conclusion has been reached for the G/L boundary claystones from the Chaotian section (He et al., 2010).

5.2. Origin of Penglaitan Group 1 sample and its implication on the Emeishan LIP

Several lines of evidence suggest that the Penglaitan Group 1 sample was derived from a mafic source. (a) As shown in Table 1, the Group 1 sample collected below the G/L boundary contains a significant amount of anatase (4.5%), a common mineral in mafic rocks. The absence of quartz and feldspar and low Al_2O_3/TiO_2 of Group 1 samples (3.7) lend additional support to their derivation from a mafic source. This interpretation is further consistent with the high contents of Fe_2O_3 and TiO_2 in the sample. (b) The Group 1 sediment displays a REE pattern similar to Emeishan basalts and has a very weak negative Eu anomaly (Fig. 3b). (c) Th/Sc ratio is another useful indicator of source rocks and is unaffected by sedimentary processes. Th is the most incompatible and Sc is the most compatible. Thus it might be expected that the ratio of these elements could represent the most sensitive index of the bulk composition of the provenance in sedimentary rocks (i.e., mafic *versus*

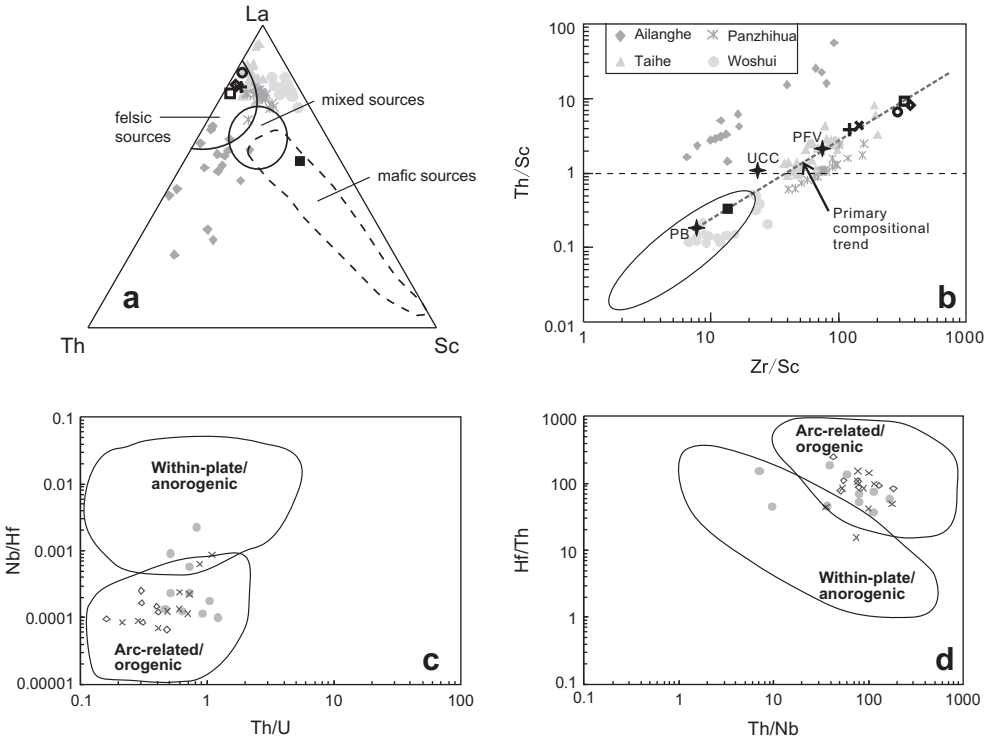

Fig. 6. Discrimination diagrams for the Penglaitan G/L boundary claystones, showing different sources for the Group 1 and Group 2 samples. (a) Ternary plot of La–Th–Sc (after Taylor and McLennan (1985)), (b) Th/Sc *versus* Zr/Sc (McLennan et al., 1993), (c) Th/U *versus* Nb/Hf and (d) Th/Nb *versus* Hf/Th for zircons from PLT-2, PLT-5 and PLT-6 (~260 Ma portion). The field in (b) outlines the compositional range of the Emeishan Basalt (Xiao et al., 2004), the discrimination fields in (c) and (d) are after Yang et al. (2012). Ailanghe: I-type granite (Shellnutt and Zhou, 2007; Zhong et al., 2011); Panzhihua: granitic intrusion (Shellnutt and Zhou, 2007); Taihe: A-type granite (Shellnutt and Zhou, 2007); Woshui: syenitic intrusion (Shellnutt and Zhou, 2007). Average Phanerozoic rock compositions (stars) from Condie (1993), PFV: felsic volcanics, PB: basalt, Upper Continental Crust (UCC) from Taylor and McLennan (1985). Symbols as in Fig. 3.

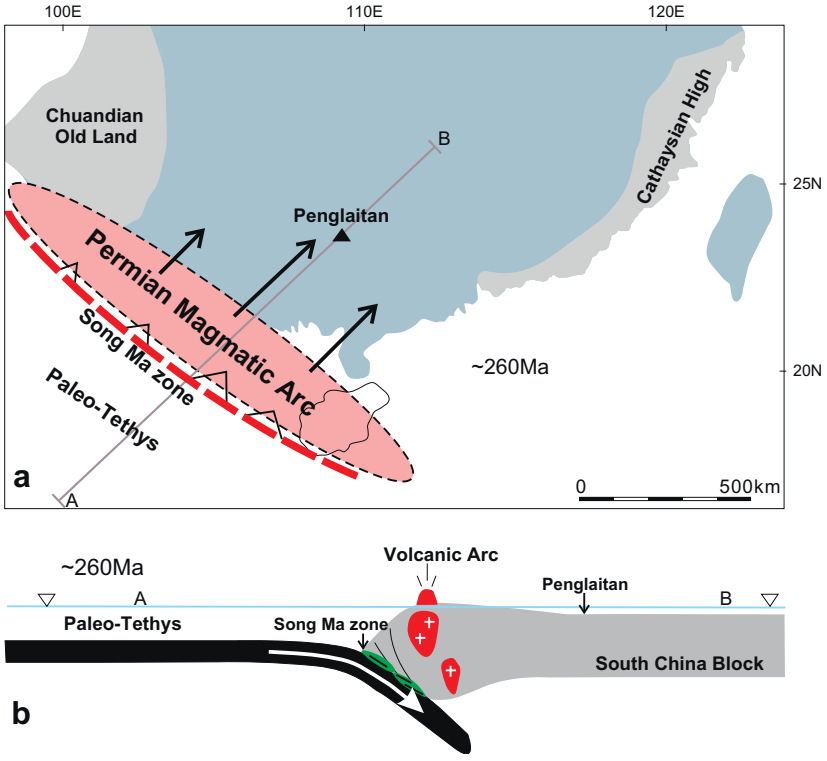

Fig. 7. (a) A sketch paleogeographical map for South China during the Permian (after Wang and Jin (2000) and Shen et al. (2011)); and (b) schematic illustration of the Permian magmatic arc formation during the Mid-Permian to Late-Permian transition (~260 Ma).

Table 5
Trace element concentrations (ppm) of zircons for claystone samples from the Penglaitan section.

	P	Ti	Y	Nb	La	Ce	Pr	Nd	Sm	Eu	Gd	Tb	Dy	Ho	Er	Tm	Yb	Lu	Hf	Ta	Th	U
PLT-2																						
1	83.1	6.7	300.6	0.8	2.7	21.4	0.8	3.3	<1.2	0.6	5.5	1.8	22.0	9.1	47.2	11.7	129.6	28.8	10699.7	0.4	84.1	222.3
2	794.6	114.7	2103.6	1.7	<0.18	5.9	0.5	6.6	11.5	<0.26	56.9	18.4	206.8	74.2	306.5	58.7	521.2	93.6	9147.3	0.9	250.5	305.9
3	213.9	29.6	470.3	4.2	3.1	15.4	0.6	3.2	3.9	0.5	14.1	4.4	47.0	15.7	64.5	12.3	112.0	19.8	8267.5	1.3	64.0	74.3
4	172.3	12.1	345.7	2.0	<0.18	18.5	<0.11	0.8	1.4	0.3	8.1	2.7	30.1	11.2	51.1	10.6	102.3	20.3	8831.0	0.8	204.1	234.5
5	219.7	11.7	721.4	0.4	<0.19	2.4	<0.09	<0.89	1.7	<0.24	13.1	5.0	64.0	24.7	110.4	22.9	208.5	39.3	9193.7	0.2	36.6	77.9
6	158.6	6.1	797.3	46.3	2.3	16.2	0.6	2.2	1.4	<0.23	8.1	3.4	50.7	22.3	124.6	32.0	346.5	71.0	8722.0	21.6	123.9	211.0
7	384.3	8.7	1405.1	2.4	<0.21	29.0	0.2	3.1	4.8	1.4	25.0	9.4	119.0	47.4	226.2	49.0	491.6	99.2	8803.1	0.7	93.7	110.5
8	156.3	27.9	501.2	2.3	1.6	14.2	0.4	2.7	2.2	0.3	8.7	3.5	44.3	16.8	77.6	16.3	154.6	29.2	9152.7	0.9	80.5	184.0
9	142.7	11.3	336.7	0.5	<0.11	11.7	0.2	<0.61	1.2	0.3	6.6	2.4	28.4	11.1	50.6	11.1	111.2	21.7	9014.7	0.3	57.6	100.9
10	237.6	5.6	556.3	5.2	7.8	38.0	1.8	7.1	3.5	0.3	10.4	3.7	46.4	17.9	85.5	19.2	196.1	38.6	9663.3	2.1	205.9	356.4
11	302.5	6.1	732.6	1.2	0.8	20.5	0.5	5.1	6.0	2.4	17.6	6.1	68.8	24.0	107.0	24.9	265.5	57.5	9060.0	0.5	198.9	154.5
12	193.2	12.4	446.6	1.0	<0.14	7.2	<0.10	0.8	1.6	0.3	9.1	3.2	39.2	14.8	68.1	13.6	132.7	25.9	8704.7	0.4	91.0	145.0
13	388.5	2.9	1099.8	7.4	0.8	14.1	0.2	1.8	2.6	<0.26	16.4	6.8	89.2	36.7	176.8	38.5	380.6	75.1	10329.2	3.0	252.9	653.4
14	256.9	6.9	951.9	1.3	0.2	2.8	0.1	1.6	2.7	<0.20	18.1	7.0	83.4	32.4	145.3	29.8	276.1	52.5	9142.0	0.7	106.0	266.4
15	198.4	<5.60	581.6	1.0	0.1	6.5	<0.11	0.9	1.7	0.3	10.6	3.9	50.9	20.0	89.2	19.0	180.4	35.0	8536.9	0.5	76.2	165.8
16	261.0	14.5	1171.9	1.8	0.7	26.7	0.4	4.4	7.6	1.5	31.6	10.7	114.1	40.1	171.2	33.2	303.2	56.6	8366.0	0.6	133.2	133.5
17	365.6	6.2	630.1	1.6	<0.12	8.2	0.1	0.9	2.9	0.6	15.9	5.7	60.1	20.8	88.4	19.1	193.9	37.6	11301.0	0.9	83.8	390.2
18	252.9	26.2	461.6	1.5	0.5	20.6	0.3	2.6	3.6	0.8	15.0	4.5	45.2	15.6	65.3	12.4	116.2	21.4	8976.5	0.4	131.3	123.5
19	107.1	26.6	254.3	1.6	2.4	8.3	0.5	2.0	1.2	<0.17	5.7	2.0	23.1	8.8	38.6	8.2	79.8	15.0	8438.3	0.4	47.4	101.0
20	368.9	13.8	723.0	0.5	<0.21	1.9	<0.15	1.3	2.8	<0.14	18.5	6.2	66.9	24.1	101.9	20.1	183.1	33.9	10214.3	0.3	54.2	218.3
21	424.3	10.2	803.4	0.6	<0.15	1.5	0.1	1.2	4.7	<0.36	23.0	7.7	80.0	26.9	106.9	20.6	184.8	34.7	10686.8	0.4	84.3	453.1
22	1053.1	3.6	1062.3	2.2	3.7	16.1	1.4	8.1	5.4	1.1	23.0	8.3	94.2	35.3	150.9	31.4	302.4	58.8	8870.0	0.8	113.6	378.0
23	132.9	<3.14	116.8	0.2	<0.13	3.6	<0.09	<0.47	0.7	0.2	2.2	0.7	8.8	3.6	17.7	4.1	46.7	–	9425.4	0.1	16.2	67.7
24	592.0	<6.41	1297.1	1.1	<0.22	1.4	0.2	1.6	4.0	<0.45	24.5	8.8	111.7	44.4	202.9	42.4	400.4	77.6	8791.2	0.5	82.0	200.9
25	166.5	9.4	718.5	3.3	<0.18	9.6	<0.16	1.9	3.4	0.2	17.5	5.7	67.4	25.5	109.9	21.9	206.3	38.2	9414.4	0.9	26.2	38.8
26	133.7	19.3	655.0	0.2	<0.12	4.0	0.3	4.6	6.2	0.9	21.6	6.5	66.8	22.9	94.9	18.3	168.9	31.9	8381.4	0.1	93.9	74.7
27	302.0	13.4	831.2	1.2	0.2	8.4	0.1	2.1	3.4	1.1	17.8	6.2	73.2	28.6	130.7	27.2	269.7	53.8	7577.6	0.4	43.9	66.4
28	187.6	16.7	443.4	1.2	19.8	60.8	5.3	19.5	4.3	0.6	11.5	3.6	41.0	14.8	66.4	14.2	140.9	27.2	8067.9	0.3	19.0	24.3
29	183.1	5.6	608.0	1.4	0.3	30.0	0.2	1.1	2.0	0.9	11.8	4.1	49.2	19.0	88.9	19.8	203.7	41.5	9331.1	0.5	152.6	204.1
30	952.0	15.6	2262.9	0.8	<0.43	1.6	<0.18	2.2	5.0	<0.54	35.4	15.0	188.0	74.7	338.5	68.3	623.3	117.1	9505.7	0.4	103.3	335.1
31	570.0	5.2	829.6	1.9	3.9	30.3	1.2	4.9	3.2	0.5	11.1	4.4	57.5	25.4	133.5	33.1	366.7	81.5	9327.1	0.7	135.8	161.6
32	676.6	27.7	1726.9	1.4	0.3	10.7	0.3	2.9	5.7	0.4	33.7	12.6	152.8	58.4	257.6	52.6	486.2	91.3	9148.3	0.7	213.6	259.0
33	247.1	22.1	339.8	0.9	0.3	12.8	0.3	4.3	6.9	0.3	21.1	5.0	40.7	11.0	41.2	7.3	63.8	11.0	11491.1	0.4	192.4	255.5
34	189.2	6.9	484.4	2.2	0.2	20.7	0.1	1.3	2.6	0.4	12.6	3.9	43.7	16.3	71.9	14.8	146.6	27.8	8387.1	0.5	47.6	59.8
35	252.5	5.9	348.3	1.1	<0.13	1.3	<0.16	1.1	3.4	0.4	19.3	6.0	45.3	11.0	34.1	5.2	37.1	5.5	12030.4	0.5	109.3	938.9
36	1081.6	6.4	939.0	1.3	11.3	43.2	2.9	14.5	4.9	1.0	17.3	5.9	74.8	30.6	146.4	33.6	351.0	74.3	7939.5	0.5	118.4	134.9
37	404.0	5.6	752.6	1.7	2.6	26.9	0.7	3.8	2.8	0.8	10.6	3.8	53.2	23.3	122.1	30.0	329.0	74.6	9285.7	0.7	117.4	153.7
38	133.7	12.9	293.7	0.9	0.8	11.7	0.3	1.8	3.1	0.9	9.0	2.5	25.1	9.0	44.7	10.9	124.3	27.9	8340.9	0.3	50.2	73.5
39	4279.2	14.7	792.7	0.9	58.3	146.7	19.3	94.1	21.9	2.9	31.8	8.1	77.0	27.4	117.4	24.3	229.6	46.3	7565.5	0.4	39.3	50.6
40	203.2	81.9	433.6	1.0	<0.32	25.6	0.2	3.0	3.8	1.2	14.0	4.3	44.5	14.8	58.6	10.9	102.9	18.1	6215.5	0.3	45.3	26.2
41	230.3	6.0	717.4	1.4	<0.23	7.1	<0.13	1.0	1.4	0.7	8.6	3.5	48.5	21.4	115.5	29.1	338.1	82.1	8702.8	0.6	79.4	263.2
42	151.9	8.3	293.2	1.1	<0.16	24.6	<0.12	0.8	1.1	0.5	5.2	1.8	22.5	9.2	44.1	10.4	115.4	25.1	9645.4	0.5	61.8	76.4
43	418.0	11.2	757.0	0.8	<0.11	3.0	0.1	2.1	3.6	0.2	19.3	6.8	73.3	25.7	104.4	19.9	174.1	30.9	10544.7	0.4	185.0	195.8
44	206.3	8.9	504.5	2.2	1.7	33.4	0.6	3.5	2.0	0.7	9.8	3.3	38.8	15.6	77.8	18.6	202.7	42.9	8839.4	0.6	239.8	202.6
45	151.2	5.6	385.3	0.7	0.2	4.1	<0.12	<0.92	<0.78	0.4	5.1	1.8	23.9	10.9	63.7	16.3	193.9	49.7	8205.3	0.4	46.9	152.4
46	272.6	9.6	631.2	1.9	2.0	18.5	0.6	3.1	2.7	0.4	12.5	5.0	57.2	21.4	94.4	19.6	177.9	33.0	9143.9	0.8	141.8	208.7
47	796.2	6.1	1840.4	0.6	0.8	7.1	1.6	12.6	8.4	1.2	29.5	12.0	159.3	62.1	283.8	58.8	542.3	100.5	10472.0	0.5	91.0	440.8
48	242.1	10.6	586.3	1.9	<0.16	13.1	0.3	3.5	4.0	0.8	17.0	5.3	58.4	20.3	82.5	16.5	152.0	26.8	8972.8	0.7	176.1	220.5
49	517.3	31.0	522.7	2.0	20.8	67.2	5.1	21.2	7.1	0.9	17.6	5.0	52.3	17.5	73.2	14.7	137.1	25.1	8834.7	0.7	176.1	168.6
50	274.4	22.1	466.2	0.9	1.2	6.7	0.4	2.2	2.7	0.7	13.8	4.4	44.6	15.9	64.5	13.1	119.5	22.1	9208.5	0.4	61.9	91.5
51	99.6	2.1	197.7	0.9	<0.11	1.8	<0.06	0.4	0.6	<0.176	3.0	1.1	14.6	6.0	30.6	7.4	77.1	16.0	9685.8	0.4	39.2	247.0
52	560.1	66.0	959.6	1.9	0.2	12.8	0.3	2.3	4.2	1.2	20.8	7.6	85.5	32.4	143.6	30.7	304.1	59.0	9259.9	0.9	96.1	174.6
53	820.3	42.9	1545.2	1.3	2.2	10.3	1.0	9.2	15.3	10.6	63.0	19.5	180.5	52.5	193.2	36.6	319.7	59.3	9002.9	0.5	89.2	216.0

54	311.2	18.0	1009.4	1.4	0.6	5.3	0.2	3.3	4.3	0.6	21.6	7.8	93.5	35.7	156.0	31.7	297.0	58.1	7770.8	0.6	112.7	189.0
55	656.5	6.0	453.0	1.0	3.8	17.5	1.0	4.1	2.2	0.5	7.0	2.6	31.7	13.0	71.2	17.3	200.0	46.1	7440.2	0.4	110.2	226.1
56	556.5	5.8	844.5	1.9	3.1	18.4	1.0	4.2	3.0	0.9	13.8	4.9	63.4	26.8	129.9	30.6	318.3	68.3	8697.2	1.0	219.1	316.5
57	243.9	8.8	924.3	1.4	0.3	10.9	0.4	3.0	3.6	1.3	21.5	7.1	81.8	31.1	136.5	28.6	271.1	53.8	7441.0	0.6	132.3	196.6
58	120.7	4.1	210.9	0.6	0.2	8.2	0.1	0.5	1.1	0.4	3.4	1.3	15.7	6.4	32.0	7.9	87.6	19.4	8919.6	0.3	107.3	223.2
59	23606.5	40.9	891.9	1.2	453.1	1252.3	174.0	833.5	181.9	4.7	160.1	24.2	141.7	32.7	99.4	16.7	140.2	25.4	10481.2	0.6	135.1	292.3
60	404.8	15.8	535.0	1.0	4.1	21.2	0.9	5.6	2.9	0.6	11.0	4.1	44.0	17.5	80.4	17.4	174.0	34.9	8301.2	0.5	84.6	148.8
61	246.0	24.4	321.8	1.0	<0.14	17.6	0.2	3.1	3.4	1.3	11.4	2.8	30.2	10.1	44.1	9.7	99.2	20.4	5234.2	0.4	140.5	195.5
62	605.9	102.0	582.0	2.3	0.8	16.9	0.4	3.3	3.4	0.7	13.1	4.6	50.5	19.3	86.1	17.7	166.8	32.0	7880.9	1.0	207.7	351.5
63	489.3	9.6	952.7	1.7	3.1	25.5	1.1	5.9	5.8	1.9	20.2	7.3	84.9	32.9	150.2	31.3	309.0	61.8	8513.3	0.6	91.8	82.5
64	1043.1	26.6	2879.9	0.9	0.8	8.5	1.7	21.2	69.2	25.3	253.0	55.7	400.0	95.6	295.9	48.2	386.9	65.0	9105.9	0.3	217.2	129.5
65	349.6	13.0	1878.0	1.0	2.6	23.6	0.6	5.7	7.4	2.2	43.8	14.7	170.9	63.0	262.8	51.5	452.9	82.4	8524.0	0.5	252.0	214.6
66	260.2	9.0	605.4	1.3	1.3	6.0	0.3	2.2	3.3	0.4	13.6	5.0	56.1	20.6	89.2	18.6	175.7	33.4	9628.4	0.6	123.9	253.7
67	484.3	8.7	1902.8	2.4	14.8	38.7	4.0	20.4	16.4	4.2	55.7	18.1	200.3	67.4	283.2	54.4	485.1	89.4	8192.3	1.2	322.9	597.5
68	306.8	19.1	1448.0	1.9	0.5	8.3	0.2	2.8	5.0	1.0	26.7	10.0	124.3	49.6	225.7	47.6	453.8	90.9	7201.1	0.5	74.1	151.1
69	171.1	25.0	373.5	0.8	0.9	3.7	0.3	2.2	3.3	0.6	10.7	3.4	35.3	12.7	53.1	10.9	104.9	20.1	6860.0	0.3	43.2	126.7
70	817.4	16.1	1805.3	3.3	1.0	9.2	0.7	4.5	9.4	3.3	44.0	17.6	190.0	62.7	259.7	52.4	480.8	85.0	10596.1	3.7	291.6	730.4
71	593.8	7.6	1427.1	1.1	<0.26	1.3	<0.12	2.0	3.7	<0.32	24.4	10.8	130.3	47.2	205.6	41.6	379.0	68.8	10434.5	0.9	138.3	547.6
72	256.4	7.4	554.4	0.9	0.2	8.5	0.2	0.9	1.7	0.5	6.9	2.7	35.4	16.7	87.8	21.3	231.6	53.6	7661.9	0.3	101.9	117.0
73	259.9	6.5	405.7	1.4	<0.11	5.0	<0.09	0.6	1.8	0.3	8.8	3.4	37.8	13.4	53.7	10.3	91.5	17.0	10314.4	1.0	115.5	419.7
74	379.7	6.2	837.3	1.6	0.4	10.2	0.5	1.5	3.1	1.2	19.4	5.8	70.0	27.7	123.5	27.9	280.2	60.3	7280.2	0.4	98.3	107.0
75	206.4	36.1	505.8	2.6	4.7	15.9	1.3	6.1	3.1	0.2	11.1	3.9	45.6	17.5	75.1	15.3	137.5	26.2	8528.8	1.0	100.1	188.3
76	266.3	9.1	388.7	0.6	0.9	9.0	0.8	5.9	7.9	1.8	21.6	5.6	44.5	12.7	51.6	10.5	114.0	23.6	9368.1	0.3	49.9	193.0
77	321.6	6.9	625.3	0.8	0.2	3.1	<0.11	1.7	3.7	0.3	17.5	6.4	67.2	20.1	72.8	12.4	104.4	17.2	10060.7	0.5	117.1	421.1
78	150.8	8.8	449.4	2.0	<0.135	32.4	0.2	1.4	3.1	0.6	10.7	3.6	38.7	14.9	66.7	14.8	147.9	30.7	8712.2	0.7	108.1	114.2
79	389.5	5.7	732.8	2.9	0.3	12.9	0.1	1.2	1.7	0.3	9.8	4.6	55.4	23.2	114.9	27.1	291.0	60.9	10890.0	1.4	76.3	379.2
80	133.0	7.6	122.4	0.9	0.2	5.9	0.9	1.7	2.9	<0.14	8.5	2.0	15.7	4.0	13.5	2.7	24.2	4.6	9615.4	0.5	176.4	192.5
81	313.7	9.5	986.2	1.7	0.9	17.1	0.4	2.7	3.6	0.9	16.9	6.4	78.5	31.3	153.9	34.7	350.3	71.9	8006.1	0.7	106.1	159.2
82	143.5	4.9	349.2	5.0	<0.21	3.2	<0.14	0.4	1.4	<0.20	4.9	2.4	30.6	12.5	56.2	11.5	114.3	22.2	10505.5	2.8	32.7	155.8
83	170.8	10.9	811.7	0.9	<0.17	4.4	0.3	3.9	8.1	1.3	27.4	7.7	75.5	26.2	112.4	22.0	212.8	41.2	6768.9	0.3	167.1	450.2
84	177.4	8.4	570.0	1.0	<0.08	6.5	<0.08	1.7	2.4	0.3	10.7	4.2	50.7	18.9	84.7	18.6	183.7	36.3	7805.9	0.5	95.0	161.7
85	839.0	4.3	2579.2	2.7	2.8	61.6	1.4	10.2	11.6	4.1	56.3	18.0	225.1	86.3	397.4	84.6	823.9	161.4	7788.4	0.6	189.9	190.7
86	261.4	14.0	1271.9	1.4	0.5	5.7	0.3	4.3	6.8	0.5	33.8	10.9	122.4	45.1	185.3	36.3	323.2	59.4	7675.6	0.7	160.9	286.3
87	1268.2	3.8	520.8	2.1	5.7	28.4	2.4	13.7	5.7	0.7	13.2	4.2	46.8	17.3	79.4	17.3	164.0	31.6	8208.2	0.8	118.2	222.2
88	1283.7	4.2	991.8	3.7	25.0	76.7	7.6	34.7	10.7	1.2	22.4	7.0	80.2	32.5	157.1	34.3	342.3	69.5	8631.5	1.4	210.1	439.3
89	267.5	5.9	809.6	2.1	<0.20	11.5	<0.09	<0.73	2.5	0.4	14.8	5.4	71.1	27.5	128.8	26.4	252.4	49.0	8723.4	0.8	80.2	148.9
90	315.5	9.7	895.5	1.8	<0.12	11.9	0.2	3.5	5.8	0.9	27.0	8.4	89.2	30.7	126.0	24.1	215.3	38.5	8076.3	0.6	75.9	71.4
91	174.0	18.4	715.2	2.5	0.2	8.1	0.2	3.3	4.8	0.1	19.4	6.2	69.2	25.7	107.5	21.0	192.6	35.4	8309.3	0.8	44.1	55.8
92	166.8	21.6	324.3	0.9	<0.12	6.6	0.1	0.9	1.7	<0.13	8.3	2.2	29.3	10.8	47.4	9.4	87.7	16.6	8745.8	0.4	50.4	87.1
93	159.5	12.7	581.1	1.5	0.2	4.2	0.2	2.2	3.2	0.3	16.7	5.3	57.2	20.1	83.6	16.7	154.0	28.7	8012.7	0.5	36.0	162.4
PLT-5																						
1	361.0	38.6	843.2	0.9	5.4	19.2	1.7	13.5	11.5	2.8	43.0	12.8	106.4	29.1	102.0	18.4	155.6	27.9	6858.8	0.3	108.7	110.7
2	232.1	11.2	807.4	4.7	6.4	34.1	2.9	15.5	8.6	2.1	24.6	7.6	75.3	27.0	118.1	24.3	234.5	44.2	8949.2	2.3	319.9	668.0
3	3730.0	6.9	1847.5	22.5	603.4	1440.1	182.8	866.7	195.4	2.1	202.3	35.0	252.7	69.5	244.9	43.6	367.8	62.7	9013.4	5.5	209.3	186.7
4	1134.9	16.4	648.8	2.3	49.3	115.6	14.1	63.0	14.5	0.5	21.8	6.4	60.7	21.6	97.7	20.6	206.4	39.6	8599.0	1.1	177.8	378.5
5	268.7	15.2	882.5	0.6	1.8	16.4	0.7	6.2	6.3	1.4	26.0	7.9	87.6	30.3	127.0	25.3	227.4	42.3	7999.7	0.3	53.7	59.6
6	6129.3	10.0	779.5	1.5	86.0	218.9	27.3	128.1	28.4	2.4	37.6	7.9	76.2	26.3	113.8	25.2	246.2	47.3	8610.0	0.5	60.7	80.5
7	224.2	73.5	573.9	2.7	8.7	23.0	2.5	10.5	4.3	<0.19	13.7	4.3	53.8	20.1	88.6	17.5	165.5	30.1	7532.2	0.8	58.6	128.0
8	187.3	8.5	660.9	2.6	<0.19	12.4	<0.11	1.2	1.4	0.4	12.1	4.6	58.4	22.9	102.2	21.9	200.8	39.8	8966.7	1.1	99.9	223.0
9	150.3	3.9	1118.6	1.2	0.2	11.2	0.3	3.9	6.3	1.8	22.7	7.0	87.8	33.5	168.5	41.1	462.7	106.1	7220.1	0.7	567.9	658.0
10	1845.9	30.5	2758.0	0.8	1.8	7.4	1.1	7.3	7.5	0.3	36.7	16.2	218.8	90.3	427.5	90.1	849.0	157.8	10405.3	0.3	44.1	335.1
11	106.6	22.2	261.2	1.0	0.9	4.3	0.2	1.3	1.6	0.3	7.4	2.5	24.4	8.6	38.7	7.9	76.6	15.3	6825.0	0.2	13.9	32.1
12	1746.3	16.3	380.0	0.9	93.0	316.7	46.7	232.4	50.5	1.0	27.4	4.3	37.0	12.0	53.0	12.0	132.3	28.5	9632.2	0.5	301.1	367.1
13	203.9	55.9	366.0	0.9	0.6	12.1	0.3	1.8	1.2	0.3	6.7	2.6	30.8	11.5	52.6	11.7	125.9	25.8	10127.0	1.7	47.7	242.8
14	129.1	49.0	405.2	4.6	5.2	17.8	1.2	4.9	2.7	0.3	9.6	3.2	36.4	14.1	61.2	12.7	121.6	23.4	7989.8	0.9	18.9	34.8
15	345.0	15.4	1265.4	5.1	1.0	23.8	1.5	13.4	17.9	6.9	53.2	15.1	141.4	42.0	171.2	33.7	311.1	59.5	8636.4	2.4	615.9	635.9
16	207.2	9.5	855.8	0.9	<0.17	10.0	0.1	1.3	2.9	0.6	14.3	4.9	64.3	27.3	126.1	28.3	285.5	59.3	8275.6	0.4	122.1	240.8
17	532.0	16.7	1478.8	2.7	6.7	22.9	2.5	14.6	10.3	2.6	45.3	13.9	153.1	53.3	214.6	41.4	373.6	67.1	7456.3	0.9	112.2	121.7

(*continued on next page*)

Table 5 (*continued*)

	P	Ti	Y	Nb	La	Ce	Pr	Nd	Sm	Eu	Gd	Tb	Dy	Ho	Er	Tm	Yb	Lu	Hf	Ta	Th	U
18	81.4	14.7	256.8	0.3	<0.22	3.8	<0.14	<0.84	0.9	0.4	5.1	1.8	21.0	8.0	40.1	8.4	86.2	17.5	6483.8	0.1	19.4	16.3
19	152.6	8.1	772.6	4.2	1.2	32.3	1.2	5.6	5.3	1.2	14.2	4.9	58.3	24.5	116.6	27.6	296.4	63.7	9138.1	2.0	255.3	505.4
20	185.9	3.9	644.4	1.4	<0.22	5.4	0.1	1.6	2.2	0.9	14.0	4.8	57.6	22.1	99.2	20.1	199.0	41.1	6934.8	0.5	45.5	75.8
21	1225.9	114.2	702.5	2.2	14.7	44.7	5.2	29.7	9.3	1.5	24.4	6.9	72.6	24.4	96.3	19.1	163.6	30.1	7527.2	0.6	64.9	44.3
22	147.8	5.6	405.9	3.5	<0.22	8.9	0.2	<0.67	0.9	<0.21	5.3	2.2	30.2	13.1	64.4	15.2	154.5	30.8	9830.0	2.0	89.2	254.6
23	182.4	5.3	650.0	1.9	0.3	25.7	0.9	8.1	8.0	3.3	27.1	7.5	71.7	21.4	90.1	16.9	160.9	29.9	7739.1	0.6	144.3	251.2
24	518.4	33.6	1062.6	0.9	0.5	1.8	0.2	2.1	3.9	0.3	26.8	10.3	105.9	34.1	132.8	25.1	223.6	39.9	11211.5	0.5	50.9	374.1
25	150.9	10.6	636.7	5.7	1.0	9.5	0.4	2.7	2.8	0.3	14.0	5.1	60.8	22.4	100.2	20.0	182.1	34.4	9859.7	2.0	46.8	93.6
26	420.5	47.5	396.9	1.2	111.1	346.5	47.9	218.5	42.5	0.9	31.7	5.0	37.9	11.8	56.0	12.6	141.6	32.5	10766.4	0.4	259.2	357.4
27	151.4	40.4	1836.2	27.4	0.2	18.1	0.2	3.2	6.4	0.4	32.5	13.1	165.0	64.0	284.1	57.4	510.2	88.9	9383.9	8.3	240.2	365.7
28	450.2	146.7	1098.8	1.7	5.7	18.9	2.2	14.7	11.2	2.4	39.7	12.2	120.2	40.4	159.1	29.3	263.3	46.7	7527.3	0.6	89.8	124.6
29	78.0	6.3	140.9	1.7	<0.21	26.2	<0.17	1.7	2.3	0.7	3.9	1.1	11.7	4.1	18.4	4.5	49.5	11.6	8891.0	0.5	167.7	617.8
30	665.4	11.7	1109.1	2.9	0.1	6.6	<0.15	1.4	3.2	<0.25	20.5	7.3	90.1	37.2	172.4	36.4	362.9	72.4	10500.7	1.2	116.2	586.6
31	528.1	9.6	1824.4	2.4	0.5	32.0	0.4	3.7	5.0	2.7	28.9	11.5	142.6	58.3	284.2	62.9	645.7	131.8	7447.1	0.5	129.5	114.8
32	141.8	8.6	646.4	1.0	<0.17	5.8	<0.172	1.9	3.1	<0.29	17.1	5.1	61.1	21.9	97.1	19.7	185.1	35.9	7183.9	0.4	92.9	162.2
33	3477.2	218.4	550.2	2.2	6.0	33.4	4.5	28.9	11.0	1.3	20.2	5.0	50.5	18.1	80.9	17.8	173.5	34.0	7889.0	0.6	43.9	85.7
34	407.4	8.5	981.7	1.2	<0.22	4.5	0.8	2.4	3.9	0.4	21.9	8.0	91.9	33.6	144.5	28.6	247.2	45.2	9619.7	0.5	163.3	165.2
35	412.2	8.6	485.3	0.4	1.4	9.5	0.6	3.5	1.4	0.7	9.8	3.3	35.9	15.7	74.8	17.2	180.4	39.7	7889.7	0.2	39.9	56.5
36	287.7	8.4	923.3	2.1	1.3	15.1	0.5	4.7	4.8	0.8	22.9	7.3	86.9	32.4	142.8	28.3	259.3	50.9	8257.4	0.7	105.2	153.8
37	1086.3	8.4	2088.1	0.9	0.9	3.7	0.3	2.2	3.2	<0.23	29.0	13.1	172.0	68.9	317.1	66.4	611.4	115.2	10284.1	0.5	67.5	318.0
38	683.4	10.2	741.2	2.9	31.1	76.2	8.0	37.5	9.1	0.3	23.1	6.7	71.7	26.0	107.8	21.4	191.0	35.9	8983.5	1.2	185.0	259.4
39	156.4	4.6	384.6	0.7	<0.21	9.1	<0.12	0.9	1.0	<0.25	6.2	2.2	26.5	12.0	59.6	14.5	156.5	34.4	9852.6	0.4	82.7	144.1
40	468.9	15.3	770.5	0.9	0.3	4.2	0.2	<1.06	2.0	<0.31	13.7	5.7	67.3	25.7	113.3	22.8	218.3	41.4	9863.9	0.5	82.6	281.5
41	237.3	16.4	670.4	2.5	<0.19	3.7	<0.09	1.1	2.3	0.6	14.5	5.5	62.0	22.8	102.2	20.8	195.7	38.4	8235.1	0.8	72.6	146.6
42	171.0	3.8	718.2	1.0	<0.23	28.3	0.6	8.1	11.6	2.1	34.3	8.2	77.3	24.7	96.0	18.7	165.6	31.5	8092.6	0.5	133.0	136.9
43	571.8	<4.49	1412.8	1.6	<0.31	8.8	0.2	3.6	6.9	<0.26	33.3	11.9	133.1	48.5	209.6	40.6	359.3	66.1	9671.9	0.9	313.8	371.6
44	559.8	8.8	1663.1	2.7	0.5	34.0	0.2	3.0	5.0	2.1	30.4	11.2	139.7	55.5	258.0	55.0	530.0	101.8	7692.3	0.7	96.2	99.0
45	850.5	97.9	938.9	1.9	6.0	48.5	2.0	12.6	8.7	1.8	29.2	9.1	92.7	32.4	132.2	25.8	243.0	44.8	6685.8	0.4	152.6	105.0
46	548.4	13.9	1464.4	1.7	0.4	24.8	0.3	2.7	4.0	1.7	22.9	8.7	113.8	47.0	231.5	51.2	516.1	106.8	7413.2	0.4	65.5	73.0
47	167.7	11.5	511.2	1.2	<0.10	11.5	0.3	0.8	1.4	0.5	8.3	3.3	40.2	16.5	78.3	17.6	180.8	37.3	8214.1	0.5	51.2	67.9
48	770.6	8.2	1825.3	0.9	0.2	1.5	0.2	1.1	3.0	<0.09	25.2	11.0	150.1	60.5	281.2	59.7	555.6	105.9	10471.6	0.5	107.8	380.4
49	367.4	30.6	1579.0	1.3	1.3	14.3	0.7	5.7	7.2	2.3	36.5	12.5	145.6	55.3	243.1	49.8	468.7	92.5	7287.7	0.4	72.1	83.6
50	363.6	2.7	1000.7	1.2	0.3	13.9	0.2	2.3	3.5	1.1	17.1	6.2	77.2	31.9	157.7	37.5	395.0	87.4	8912.1	0.4	106.2	177.9
51	143.5	4.8	640.0	2.4	0.1	5.3	<0.07	1.6	3.9	0.2	16.5	5.8	59.5	19.9	87.0	17.5	166.9	32.9	9582.5	0.9	188.7	346.3
52	293.6	14.1	811.5	5.0	0.1	20.2	0.1	2.4	4.2	0.4	21.8	7.4	79.1	27.4	115.3	23.1	210.9	38.9	9448.9	1.5	66.4	78.7
53	544.8	20.6	2052.8	3.1	0.6	60.7	0.5	5.6	9.7	5.7	51.2	16.8	197.5	72.7	313.6	63.2	582.1	111.5	7806.7	0.6	190.3	115.3
54	194.0	18.3	759.1	0.4	<0.08	11.3	0.2	2.2	5.2	1.1	20.9	6.2	69.2	25.5	111.8	23.1	219.7	42.4	9096.2	0.2	111.4	96.9
55	214.0	9.0	753.6	1.1	<0.09	9.1	0.3	4.0	5.3	0.7	21.8	6.7	73.5	26.1	108.2	21.4	196.5	37.6	7753.6	0.5	96.0	166.3
56	167.4	17.3	711.1	1.2	<0.11	6.5	0.2	2.0	3.6	0.2	17.5	5.8	65.3	23.5	102.2	20.5	187.3	35.2	9182.6	0.5	72.4	97.4
57	237.7	23.6	148.8	0.2	<0.08	4.1	0.2	3.7	6.0	0.3	15.8	3.1	21.5	5.1	13.6	2.1	15.4	2.2	9992.4	0.0	87.6	216.0
58	860.3	10.2	686.0	1.0	7.3	39.2	2.9	15.7	7.8	1.3	21.9	6.1	66.3	22.9	100.3	20.8	198.6	39.4	8158.9	0.5	76.9	91.2
59	267.0	8.2	1291.3	5.7	0.2	61.8	0.2	2.6	5.1	1.6	24.8	8.5	105.7	42.1	197.8	42.8	415.8	83.1	8439.1	1.3	179.2	157.4
60	219.8	6.5	717.4	0.7	<0.08	15.6	0.1	2.7	4.5	0.8	18.2	5.4	60.7	22.9	105.4	23.7	244.1	52.5	8428.5	0.5	190.9	299.9
61	1988.7	29.3	940.0	1.5	67.3	158.8	16.8	73.1	15.3	3.3	28.9	7.7	85.2	32.0	142.1	29.6	283.9	55.8	6198.0	0.3	113.8	116.3
62	180.7	21.5	1052.9	2.5	1.7	13.2	0.4	3.4	4.7	0.5	22.8	8.2	96.0	35.9	155.1	30.5	278.7	50.8	8625.9	0.6	48.7	76.0
63	272.8	4.8	349.3	0.5	2.0	7.1	0.4	2.1	3.2	<0.17	12.1	3.7	36.0	11.3	45.7	8.7	79.7	14.7	9368.8	0.2	98.0	251.8
64	216.9	20.4	458.8	2.4	<0.23	13.3	<0.142	1.4	2.8	2.6	12.3	3.8	43.8	15.6	67.7	13.3	121.3	23.2	8931.8	0.4	104.8	46.5
65	181.6	23.4	940.9	0.3	<0.12	4.6	0.3	3.2	4.4	1.6	18.1	6.5	77.9	31.3	144.2	30.9	303.0	61.5	6795.6	0.1	73.7	69.5
66	154.6	8.4	187.2	0.7	<0.12	1.2	<0.08	0.7	1.6	0.3	9.0	2.3	22.4	5.9	22.2	4.5	42.1	8.9	10742.6	0.4	36.2	299.6
67	228.2	8.6	295.1	0.8	<0.18	7.3	<0.13	1.0	3.1	0.3	11.4	3.7	33.0	9.7	36.3	6.8	58.0	11.2	9665.4	0.4	53.6	71.7
68	190.5	8.5	595.0	0.9	<0.23	7.8	<0.13	<0.90	1.7	0.7	11.5	3.8	47.1	19.0	93.2	19.4	200.8	40.5	7686.7	0.4	88.4	161.0
69	327.1	3.8	1248.9	6.1	1.0	62.9	0.3	2.4	3.0	0.6	17.5	7.4	94.3	39.9	193.5	42.4	414.3	82.0	8934.2	1.2	87.2	88.5
70	395.6	15.4	1277.5	0.9	3.3	16.1	2.8	20.3	17.6	3.8	51.9	14.0	136.5	45.4	178.3	33.8	302.6	56.7	7581.4	0.4	102.1	263.9
71	203.5	9.1	542.1	2.5	1.0	14.6	0.4	1.9	2.7	0.4	11.9	4.3	49.8	18.9	83.0	17.4	163.5	30.8	9822.0	1.1	146.0	279.2
72	4693.6	7.9	2063.3	4.3	58.0	187.5	18.7	90.9	24.0	4.2	48.7	15.5	176.7	69.6	319.8	70.2	687.2	136.9	9364.5	1.3	175.2	173.0
73	266.9	14.3	586.4	0.8	1.2	14.3	0.7	6.1	6.5	1.1	20.6	6.1	61.8	20.2	84.6	16.2	143.8	26.8	7437.8	0.2	44.6	48.1

74	325.9	5.3	635.1	1.0	2.5	15.1	0.7	3.7	2.7	0.8	13.4	4.7	51.2	20.2	94.3	19.8	200.2	39.0	8627.1	0.5	176.4	252.2
75	362.0	22.6	1276.9	3.0	1.1	26.2	0.4	3.9	5.2	1.5	26.4	9.1	106.5	42.7	191.0	41.4	402.3	80.1	7498.8	1.0	212.7	246.3
76	410.1	21.1	802.8	2.0	1.8	18.9	0.5	3.0	2.4	0.8	11.9	4.6	60.6	25.7	125.8	29.1	310.1	69.2	8455.6	0.7	202.0	336.9
77	641.9	7.0	1406.9	1.7	0.3	6.7	0.2	1.2	1.7	0.9	17.1	7.7	110.7	49.0	242.8	53.2	539.2	107.0	9962.7	0.8	52.7	214.4
78	586.3	8.8	732.2	2.9	36.6	95.8	10.8	54.2	13.4	0.5	29.1	7.7	76.8	26.7	110.5	21.1	191.8	37.3	9129.0	0.8	94.9	103.6
79	926.9	5.7	1872.7	0.9	<0.21	1.7	0.3	1.9	4.2	<0.20	26.8	11.6	152.8	61.6	284.6	60.4	565.7	105.5	10103.6	0.5	64.6	244.4
80	622.1	6.4	1246.3	1.6	<0.21	2.1	0.2	1.2	3.0	<0.19	18.6	8.0	105.2	41.3	189.9	41.9	391.8	76.5	9474.5	1.0	119.2	397.6
81	747.6	7.2	1381.1	0.6	<0.21	1.0	0.1	1.2	1.6	0.2	20.3	9.2	120.5	45.2	202.3	41.5	373.6	67.3	11499.3	0.5	54.4	519.4
82	310.9	11.8	519.3	0.8	<0.13	3.9	0.2	2.0	3.3	0.2	17.5	5.6	55.4	17.7	66.9	12.5	103.5	19.0	9536.5	0.4	95.7	165.5
83	262.6	7.1	893.6	1.0	0.5	6.6	0.3	1.4	3.2	0.5	17.2	6.7	84.5	31.7	137.2	28.1	262.0	51.4	8263.5	0.5	77.2	160.2
84	344.6	6.5	787.9	1.0	<0.15	2.0	<0.12	<0.93	2.3	<0.20	12.6	5.2	70.5	26.7	121.4	25.0	238.7	45.6	9056.4	0.6	77.1	222.3
85	221.5	10.1	795.5	1.0	0.7	10.7	0.4	4.0	5.8	1.2	21.0	7.2	77.5	27.7	118.5	24.3	231.6	44.9	7341.2	0.4	66.7	151.8
86	205.7	45.5	493.1	1.5	2.7	16.4	0.6	3.8	3.8	0.4	14.6	4.4	47.4	17.0	71.4	14.0	127.7	23.9	8443.4	0.5	82.6	67.8
87	206.1	10.3	419.3	2.9	0.2	5.6	0.1	1.1	2.4	0.1	12.1	3.9	39.1	13.3	54.1	11.2	105.1	20.2	11362.7	1.1	174.6	433.1
88	784.6	<3.71	1009.9	1.2	0.5	12.5	0.3	3.3	3.5	0.9	17.4	6.6	81.3	32.4	153.7	33.7	348.4	72.4	8485.8	0.5	154.2	256.0
89	189.2	17.4	433.9	0.7	<0.22	3.7	<0.19	1.3	2.6	0.4	9.0	3.3	38.9	14.8	63.9	14.0	133.4	25.9	8081.1	0.3	26.9	60.2
90	542.6	87.4	518.8	2.3	17.1	41.2	5.1	24.3	6.8	0.3	15.1	4.3	48.3	17.6	77.6	16.1	150.4	28.2	7392.4	0.6	46.3	107.3
91	474.9	25.4	786.7	1.8	2.2	15.0	0.9	5.7	3.7	0.3	15.5	5.4	67.3	26.4	119.5	24.7	237.0	46.1	8608.0	0.7	71.0	121.7
92	561.8	5.9	1291.0	1.8	0.2	2.4	0.1	1.5	3.3	0.3	19.5	8.3	107.3	43.9	202.4	43.7	413.6	81.7	8863.6	0.9	141.2	408.2
93	248.1	47.9	859.0	1.7	0.7	16.9	0.7	5.8	7.7	0.7	29.8	8.6	88.8	29.3	117.5	23.0	205.7	37.0	8211.0	0.6	103.2	122.5
94	638.4	6.2	1207.6	1.6	0.3	5.9	0.5	1.1	3.3	0.4	20.8	8.4	104.7	41.0	183.0	37.4	355.9	68.6	9307.3	0.8	90.4	248.4
95	302.0	11.1	929.4	2.1	<0.09	17.9	<0.09	0.7	2.2	0.4	15.4	5.9	77.7	31.4	144.8	31.4	308.5	60.1	9305.4	1.0	86.5	126.2
96	247.8	17.0	1010.5	0.4	0.2	14.3	0.3	5.3	7.1	1.2	27.0	8.5	93.0	33.9	144.8	28.9	262.5	49.9	8299.9	0.2	123.0	101.5
97	388.0	14.8	702.3	1.4	<0.11	4.5	0.2	2.0	4.3	0.2	18.1	5.9	66.3	23.0	97.0	19.4	182.1	33.5	9415.5	0.5	109.0	136.1
98	634.6	10.4	1142.9	2.0	102.4	215.4	22.2	84.5	17.9	0.2	31.1	9.9	109.8	40.1	171.4	35.0	319.5	57.7	10620.6	1.1	362.6	460.1
99	241.5	45.3	998.8	1.5	0.9	19.5	0.4	4.3	5.4	2.0	22.1	7.5	85.6	32.8	152.4	32.9	333.8	68.3	5118.8	0.2	95.2	63.1
100	248.8	14.3	602.6	0.7	0.3	12.3	0.2	2.0	2.9	0.6	13.3	4.4	52.0	19.6	89.2	18.8	186.2	36.5	8269.6	0.4	83.1	90.0
101	623.9	9.1	686.0	0.8	4.5	25.4	1.4	7.6	4.1	1.0	15.6	5.0	58.4	22.2	103.8	22.6	223.8	44.9	7890.7	0.3	72.8	78.7
102	211.0	4.1	772.8	0.6	<0.08	4.0	<0.09	0.6	1.6	0.4	10.3	4.5	58.9	25.1	123.6	27.8	280.9	58.2	8705.3	0.3	61.3	150.4
103	256.8	31.6	487.4	2.3	1.0	6.2	0.3	1.3	1.4	0.2	7.8	3.1	40.2	15.9	75.0	15.7	149.9	28.7	8255.7	1.0	34.8	72.6
104	605.3	7.9	1177.1	0.9	<0.17	2.6	<0.12	1.1	3.7	<0.23	20.2	8.0	103.4	40.1	179.4	36.6	338.9	62.6	9853.1	0.4	94.9	160.5
105	509.6	7.6	914.9	0.5	<0.13	1.1	<0.11	1.6	3.8	<0.18	25.4	8.5	91.5	30.6	124.1	23.8	212.9	38.9	8932.0	0.3	79.1	351.2
106	433.6	38.8	706.0	9.6	<0.22	11.6	0.2	3.1	7.5	0.8	37.2	9.9	83.9	23.4	90.5	17.1	158.8	29.1	10908.7	8.4	68.3	360.1
107	403.0	4.1	1186.6	8.4	2.4	77.9	1.0	6.3	8.1	1.6	20.7	7.0	86.5	35.7	179.2	41.9	442.7	91.2	9743.4	1.6	632.5	580.1
108	5410.3	11.6	228.4	0.6	101.5	209.6	22.1	85.4	13.4	1.5	15.8	3.2	25.5	7.7	28.5	5.6	50.9	9.0	7441.3	0.2	69.9	125.1
PLT-6																						
1	407.5	12.7	893.7	2.0	0.6	26.2	0.3	4.6	7.8	0.8	28.7	8.8	90.7	30.1	125.9	24.1	223.7	43.3	8322.6	0.3	165.0	74.4
2	625.6	5.9	1000.9	2.2	12.3	42.2	4.4	21.0	8.0	0.2	23.8	8.1	92.3	34.6	149.5	29.7	273.7	51.6	9286.9	1.1	246.1	485.1
3	125.9	17.6	296.7	1.7	0.3	4.6	0.1	1.1	1.5	0.6	5.9	2.1	26.5	9.8	45.5	9.7	92.8	18.5	9294.4	0.6	74.0	203.0
4	162.4	77.9	613.0	3.7	3.8	13.2	0.8	4.9	3.9	0.6	15.1	4.7	54.2	19.8	91.1	19.8	198.6	39.4	6177.3	0.9	132.6	184.5
5	553.7	675.9	1345.7	2.0	0.0	2.0	0.1	1.4	4.0	0.2	24.4	9.6	121.4	46.8	209.2	42.6	390.1	75.4	10412.0	0.6	116.1	335.8
6	126.0	6.0	199.2	0.6	0.1	17.6	0.2	1.8	1.5	0.4	6.1	1.7	17.7	6.2	28.2	6.1	59.1	12.0	8223.5	0.2	16.9	19.8
7	268.3	13.3	685.2	1.9	<0.05	6.3	0.1	1.1	3.0	<0.09	13.5	5.2	62.3	23.4	101.7	21.0	192.8	35.9	10577.6	0.9	161.8	146.4
8	545.3	63.0	2149.9	4.1	0.4	84.7	0.3	3.6	7.8	2.5	45.9	16.5	200.7	75.0	327.0	65.1	590.8	112.7	7446.9	1.0	121.9	104.5
9	145.0	7.4	336.1	2.1	<0.10	8.4	0.2	<0.54	1.5	0.3	7.0	2.4	27.6	11.0	52.3	11.6	115.1	23.7	9146.4	0.5	22.0	33.5
10	487.4	19.7	631.2	8.1	13.2	39.0	3.5	15.2	5.1	0.2	13.1	4.5	54.2	21.3	98.1	20.3	191.0	37.3	8711.1	2.1	56.5	111.0
11	247.8	4.9	442.6	1.0	2.3	12.8	0.5	2.1	1.5	0.6	6.6	2.4	31.6	13.8	70.3	17.4	195.6	46.6	9205.7	0.5	89.4	168.9
12	200.2	43.0	443.6	0.5	1.1	11.4	0.3	1.9	2.7	0.7	11.3	3.8	40.5	15.1	64.1	13.1	125.9	24.8	8123.7	0.2	16.1	21.5
13	53.3	3.5	176.1	0.6	<0.07	16.3	0.5	0.9	1.6	0.9	4.8	1.5	14.4	5.1	22.9	5.4	55.3	11.8	5455.6	0.2	110.0	110.9
14	354.7	35.2	957.0	3.5	<0.07	8.6	0.5	5.5	7.9	1.1	31.4	9.5	99.7	33.7	132.7	24.8	216.9	38.9	8093.7	1.3	66.7	55.2
15	184.1	33.1	508.1	1.0	1.4	6.7	0.3	1.6	2.6	0.3	11.6	4.0	46.2	17.0	76.1	15.5	145.4	27.6	7423.0	0.4	39.6	86.2
16	47.4	4.0	139.5	1.4	<0.05	23.4	0.2	0.3	0.9	0.2	2.4	0.8	10.4	4.0	20.9	5.0	57.8	15.0	8873.0	0.3	118.9	176.8
17	601.0	17.3	938.9	2.7	1.9	54.9	0.9	7.4	7.0	1.5	24.3	7.6	85.1	30.6	136.4	28.5	270.9	53.0	7619.3	1.0	313.3	313.7
18	139.0	7.6	908.7	1.4	<0.20	21.3	0.6	6.8	7.9	3.0	26.5	8.3	84.7	29.7	129.4	27.3	265.0	53.5	7990.0	0.4	113.0	109.7
19	291.5	22.9	199.1	0.1	0.2	3.4	0.3	4.5	8.3	0.2	21.2	4.0	27.9	6.7	20.5	3.3	26.7	4.1	9612.1	0.1	113.9	266.0
20	83.7	5.1	451.9	1.5	<0.07	47.3	0.5	6.2	6.7	2.0	20.9	5.3	49.2	15.1	58.7	11.5	107.5	20.4	8300.0	0.5	188.3	270.5
21	113.6	6.5	773.4	0.8	0.5	21.8	0.4	5.2	8.1	3.8	27.1	7.9	77.9	25.6	105.5	21.1	199.0	38.6	7631.7	0.4	129.5	108.9

(*continued on next page*)

Table 5 (*continued*)

	P	Ti	Y	Nb	La	Ce	Pr	Nd	Sm	Eu	Gd	Tb	Dy	Ho	Er	Tm	Yb	Lu	Hf	Ta	Th	U
22	549.7	15.9	827.9	1.7	35.2	89.4	9.8	47.2	16.4	0.7	40.6	9.8	90.4	28.6	110.3	20.3	172.4	30.9	8563.5	0.6	152.0	114.1
23	357.7	3.5	776.7	0.8	0.0	6.5	0.3	5.2	10.2	0.3	38.0	9.3	85.4	27.5	106.6	20.2	180.5	34.1	9439.6	0.2	150.1	52.2
24	723.4	11.0	1238.3	3.2	12.6	41.6	5.0	25.2	10.3	0.7	33.3	10.4	119.2	43.1	181.6	35.3	317.7	60.4	8743.0	1.1	80.7	122.2
25	490.5	4.8	214.4	0.2	6.1	23.4	1.4	5.4	1.6	0.4	5.3	1.6	18.1	6.6	32.7	7.7	81.0	17.9	8613.8	0.2	32.3	58.9
26	187.7	14.3	526.8	6.3	4.2	19.0	1.9	6.7	3.7	0.4	15.3	4.7	51.1	18.6	79.1	15.0	139.8	27.0	6812.0	1.8	41.2	92.4
27	756.5	7.4	853.2	4.6	15.6	49.4	5.1	23.7	7.6	0.4	21.1	7.0	79.2	28.8	130.5	26.1	247.7	48.0	9258.9	1.7	73.6	170.1
28	526.6	23.1	1256.2	0.5	15.6	103.6	4.6	29.0	17.4	4.8	51.3	13.6	136.1	45.7	184.6	35.3	319.9	64.8	5247.8	0.2	41.0	20.9
29	4827.6	13.9	861.7	2.6	286.4	682.6	88.8	412.8	87.6	1.3	87.6	15.3	112.1	30.7	114.1	21.2	187.5	34.2	8669.1	1.0	103.0	207.1
30	212.1	5.7	547.9	1.7	0.9	7.5	0.5	1.7	1.8	0.2	9.6	3.3	42.5	18.5	90.9	20.4	210.1	42.0	10004.7	1.2	95.3	145.6
31	199.0	13.8	840.1	1.2	0.9	5.4	0.5	4.7	5.7	0.5	24.3	7.7	82.4	28.5	117.7	23.2	205.1	38.1	7853.1	0.5	72.1	94.6
32	177.8	7.2	295.9	1.1	2.2	12.4	0.7	3.2	2.0	0.2	6.5	2.2	26.1	9.8	44.0	9.6	92.8	18.0	9732.7	0.6	104.2	124.5
33	2610.7	5.7	773.5	1.0	31.7	74.5	7.1	27.6	6.8	1.3	17.8	5.4	63.8	24.9	117.3	25.8	261.1	55.1	8901.0	0.5	118.4	130.2
34	218.3	10.6	978.6	1.5	0.2	18.0	0.3	3.5	4.8	1.7	22.5	7.1	82.5	32.1	143.6	31.0	307.8	61.7	7178.1	0.6	142.8	109.0
35	383.2	17.2	745.9	1.5	<0.08	3.7	0.1	2.0	3.8	0.1	18.5	6.3	70.0	25.2	107.0	21.3	200.8	38.0	10021.1	1.0	329.8	393.6
36	348.4	15.8	1039.5	2.9	1.7	15.2	0.6	4.4	4.5	0.5	21.7	7.5	90.9	34.1	157.1	32.2	308.7	58.5	7652.5	1.0	79.8	96.7
37	246.2	18.5	896.8	1.7	0.4	10.4	0.3	5.0	8.4	0.8	31.4	8.8	91.4	30.6	124.8	24.6	222.2	40.6	8721.5	0.5	123.2	117.9
38	464.8	11.4	1441.3	2.5	1.5	16.4	1.3	9.8	11.4	7.1	37.2	13.0	143.9	50.6	209.8	42.2	382.5	68.6	10827.4	1.1	231.4	496.8
39	40.5	4.3	252.8	3.6	0.7	4.7	0.2	0.7	<0.31	0.4	3.0	1.0	17.6	7.9	44.0	11.8	142.1	33.1	8911.1	1.2	44.3	132.4
40	496.8	21.5	567.2	0.9	99.1	73.0	9.1	29.9	7.4	1.2	16.8	5.0	53.8	19.1	78.6	16.5	151.2	28.8	8864.4	0.3	36.7	42.6
41	166.3	3.2	612.5	0.8	0.5	3.6	0.1	0.5	1.7	0.5	7.6	3.5	41.5	18.8	102.5	25.8	291.0	66.7	6903.4	0.3	13.5	36.1
42	207.4	15.4	721.6	3.6	24.3	62.0	5.5	19.9	4.8	0.3	13.3	4.9	58.8	23.3	110.9	23.8	229.5	44.7	9868.7	2.0	185.5	492.4
43	188.8	13.5	569.0	4.4	1.8	39.7	0.7	4.3	5.7	2.1	21.5	6.4	59.1	18.9	81.5	16.9	167.9	32.5	8478.1	1.3	133.9	127.5
44	128.9	16.7	302.4	1.6	0.2	14.2	0.1	1.8	2.3	0.2	8.1	2.8	29.2	10.3	44.0	9.1	84.8	16.0	9353.6	0.7	105.8	132.4
45	246.1	8.5	563.2	1.1	0.6	6.9	0.8	5.3	5.3	1.2	13.9	4.7	53.1	18.9	85.1	17.8	171.9	33.4	9616.9	0.5	79.1	290.7
46	231.0	14.1	487.9	0.7	0.7	8.5	0.8	1.4	1.7	0.4	8.7	3.4	41.7	16.2	74.7	15.8	158.5	31.5	8173.3	0.3	36.4	81.3
47	456.1	10.2	2328.3	7.9	45.0	133.8	15.7	76.9	25.7	0.9	67.4	21.3	237.4	83.2	340.6	63.9	539.0	92.9	7619.6	1.8	201.8	329.9
48	388.7	2.8	997.8	3.7	<0.07	27.6	<0.11	0.9	2.4	0.5	14.5	6.0	76.3	30.9	150.8	33.3	335.2	68.1	11135.1	1.8	227.5	308.6
49	171.6	22.1	320.2	1.3	<0.06	2.7	0.1	1.1	1.7	0.1	7.3	2.4	26.8	10.3	47.1	10.2	98.7	19.7	10126.4	0.5	75.0	101.2
50	484.0	27.6	1507.5	2.4	56.4	55.0	12.2	49.0	13.7	3.2	29.5	10.2	119.0	48.8	236.6	51.5	513.4	102.3	10423.6	1.3	373.9	663.1
51	164.3	4.9	636.2	3.1	0.9	13.8	0.2	1.4	3.0	0.1	13.6	4.9	58.0	21.3	94.8	19.3	178.6	32.3	10960.6	1.5	265.2	271.0
52	108.9	7.2	352.4	3.7	0.7	34.3	0.7	4.7	2.9	1.1	7.7	2.8	27.7	10.6	52.6	13.1	141.1	30.1	9672.4	1.2	249.6	389.4
53	83.0	9.8	368.3	2.3	0.1	13.2	0.4	2.0	2.7	0.1	13.3	4.1	39.0	12.8	51.9	9.8	86.3	15.1	9695.0	0.9	138.5	156.0
54	205.8	9.1	591.8	0.8	0.1	13.1	0.1	1.1	1.8	0.6	10.7	3.9	48.8	19.6	90.5	20.0	201.5	40.2	8684.3	0.3	55.1	64.9
55	1080.2	6.4	502.0	1.0	5.1	20.2	1.4	6.7	3.4	0.8	10.7	3.4	40.7	15.9	76.4	16.7	181.5	39.0	7595.3	0.4	56.0	89.0
56	242.0	4.8	1097.1	2.1	0.6	6.5	0.3	3.4	3.9	0.7	22.1	8.2	98.3	38.0	171.8	35.2	332.6	65.9	8406.2	0.9	170.5	378.7
57	174.3	7.8	503.6	1.2	0.3	12.9	0.2	1.9	2.8	<0.32	13.2	4.2	45.4	16.2	69.8	14.7	144.7	27.7	9495.0	0.6	204.8	430.2
58	341.6	10.6	1785.6	14.0	9.2	47.0	3.0	16.8	14.1	1.4	50.5	17.3	188.2	64.6	263.4	48.3	409.4	71.5	6145.0	3.3	133.9	163.6
59	3654.7	5.0	1317.8	1.2	213.4	534.2	72.1	357.5	80.1	2.6	96.4	19.6	161.4	50.0	189.2	34.5	301.4	56.5	5824.6	0.4	45.0	60.5
60	207.2	9.0	518.1	1.3	1.3	9.8	0.4	1.7	1.9	0.2	7.5	3.1	38.9	15.8	75.5	16.5	162.0	31.0	12254.8	0.9	184.9	245.2
61	282.6	11.6	681.8	1.4	0.1	12.6	0.2	0.9	2.4	1.3	29.6	10.3	82.5	23.7	91.0	17.4	159.7	29.3	9675.6	0.8	130.5	253.5
62	170.9	20.5	568.7	10.6	20.0	58.3	6.3	27.5	7.2	0.5	17.3	5.4	58.8	20.4	85.9	17.0	153.5	27.2	7539.4	2.6	49.0	142.2
63	686.6	9.4	1267.9	0.7	<0.11	2.1	<0.13	1.3	3.3	<0.17	20.5	9.2	111.5	41.8	182.2	37.0	332.4	61.1	10371.9	0.5	72.5	385.1
64	124.3	5.8	280.1	0.3	<0.09	9.6	<0.10	0.5	1.3	0.5	7.1	2.2	23.2	9.2	42.4	9.4	98.2	20.0	8580.2	0.3	31.2	66.8
65	172.9	9.1	565.4	0.5	0.1	8.0	0.1	1.7	2.3	1.3	12.3	4.5	49.4	18.4	83.6	17.3	163.7	33.5	7770.6	0.4	101.6	119.7
66	565.8	126.8	1907.6	3.2	2.5	20.0	3.1	24.9	22.3	4.3	56.8	18.4	191.8	64.5	264.2	49.5	430.0	74.9	9055.2	1.4	851.5	540.3
67	422.5	7.8	777.3	0.8	0.5	7.2	0.1	1.5	1.8	0.4	9.5	4.6	59.0	25.2	121.9	26.2	246.5	47.3	10252.6	0.5	53.3	261.5
68	478.8	9.6	1149.9	0.6	<0.11	2.1	<0.11	1.2	3.1	0.2	22.1	8.4	103.1	39.9	176.6	35.7	334.1	63.7	9523.3	0.3	68.3	141.5
69	270.0	6.6	467.6	1.6	<0.05	3.9	0.1	1.2	3.4	0.3	13.4	4.3	45.7	15.1	62.0	11.9	112.1	20.2	10602.7	0.9	145.0	463.8
70	440.4	8.5	890.0	0.8	<0.09	2.1	0.1	1.0	2.1	0.4	14.8	5.8	73.4	29.2	136.0	28.8	270.1	52.5	9995.7	0.6	62.8	265.1
71	550.1	10.4	1543.2	3.0	0.5	11.0	1.0	9.5	16.7	14.5	68.6	19.8	179.0	51.6	192.6	35.0	296.0	53.6	9838.5	2.0	233.2	260.6
72	155.0	17.3	218.3	1.2	<0.13	21.5	0.1	1.5	1.4	0.4	3.3	1.3	15.8	6.5	33.2	7.8	83.1	17.4	9536.2	0.6	114.8	99.7
73	407.1	12.0	1069.3	1.9	0.9	7.2	0.4	3.3	4.2	0.3	22.4	8.2	100.5	37.1	162.7	33.6	323.4	60.5	9085.7	0.5	58.5	144.6
74	264.8	9.9	1263.3	<0.03	<0.13	2.7	0.2	3.3	6.7	0.3	32.7	11.3	126.5	43.9	180.6	34.2	290.1	51.8	8134.4	0.3	61.7	129.4
75	276.7	8.6	1263.3	1.7	0.1	17.7	0.5	5.0	8.6	3.9	33.0	10.9	115.8	40.8	176.2	36.6	359.0	72.8	7399.1	0.5	139.1	196.0

76	516.1	9.7	1123.5	2.0	0.2	8.2	0.2	3.2	6.6	0.5	27.3	10.0	108.9	38.8	163.1	32.1	290.8	54.0	9490.7	1.2	272.3	443.9
77	389.1	5678.4	606.0	165.9	110.5	252.5	31.7	149.9	33.8	6.2	37.9	7.7	68.4	22.2	89.7	16.8	158.0	28.5	6976.8	14.5	51.8	70.4
78	150.6	13.1	403.1	1.7	0.2	8.8	<0.07	<0.59	1.7	0.3	8.8	3.0	36.4	13.9	60.7	12.1	115.6	22.0	8255.0	0.7	95.0	161.3
79	547.8	<2.07	318.3	1.6	4.1	20.4	0.8	2.1	1.2	0.7	5.2	1.7	21.3	8.9	47.3	12.1	144.8	37.5	9158.9	0.2	137.5	128.4
80	203.0	40.7	943.5	1.5	1.0	22.0	0.6	4.8	8.0	3.9	33.3	9.3	91.0	31.0	137.2	28.4	287.3	58.3	9185.0	0.6	346.8	706.8
81	305.5	5.3	859.2	1.5	8.5	27.0	2.6	14.7	7.8	0.5	28.1	8.2	84.3	28.8	121.8	23.4	215.0	39.6	8089.9	0.5	74.6	101.3

felsic component; Taylor and McLennan, 1985; McLennan et al., 1993). On a La–Th–Sc ternary diagram (Fig. 6a), which is commonly used to discriminate felsic and mafic provenance of clastic sedimentary rocks (e.g., Taylor and McLennan, 1985), Group 1 sample falls into the mafic source area.

Laibin is located about 800 km southeast of the ELIP (Fig. 1), and the Laibin Limestone is the uppermost part of the Maokou Formation. Therefore the ELIP is a possible source for the Group 1 sample. Moreover, mineralogical and geochemical analyses suggest that the Group 1 sediment is probably from the basalts of the ELIP. This conclusion is in good agreement with Wignall et al. (2009b) who found the sub-mm sized basaltic pyroclasts within Laibin Limestone of the *Jinogondolella granti* Zone at the Tieqiao section. Considering the long distance between Laibin area and Emeishan LIP, the Emeishan volcanism with unusually violent eruptive style was under way at least by the *Jinogondolella granti* Zone (Wignall et al., 2009b). The claystone PLT-1 (Group 1) was from the horizon about 60 cm below the G/L boundary (Fig. 1b), which is exactly in the topmost part of the *Jinogondolella granti* Zone. Thus, the causal link between G/L mass extinction and Emeishan volcanism is confirmed because of this remarkable coincidence. No pyroclasts or volcanic clasts have been found above the G/L boundary at the Penglaitan section (see Fig. 5 in Wignall et al., 2009b). Consequently, the main phase of the Emeishan volcanism may have terminated prior to the G/L boundary, as already suggested by He et al. (2007, 2010).

5.3. Provenance of the Penglaitan Group 2 claystones

The Group 2 samples possess a relatively high content of quartz, pointing to an affinity akin to felsic sources. According to Hayashi et al. (1997), Al_2O_3/TiO_2 ratio increases from mafic rocks (3–8), via intermediate rocks (8–21) to felsic rocks (21–70). The relatively high Al_2O_3/TiO_2 ratios (20.7–33.2) of the Group 2 samples are consistent with a derivation from an intermediate to felsic source. This is further supported by the presence of strong negative Eu anomalies (0.18–0.47, Fig. 3b), and plot of these samples within the field of typical felsic source area in the La–Th–Sc ternary diagram (Fig. 6a). On the Th/Sc *versus* Zr/Sc diagram (Fig. 6b), all samples (Group 1 and Group 2) are distributed along the primary compositional trend defined by average Phanerozoic rock compositions. We thus suggest that the Group 2 samples are likely derived from a felsic component source.

Paleogeographically, the Laibin–Heshan area was a part of the Dian-Qian-Gui Basin (Fig. 7). Three possible sources (i.e. Cathaysia Block, Chuandian Old Land and northern margin of palaeo-Tethys) can be proposed for the Group 2 claystones.

Chuandian Old Land or the Emeishan LIP is mainly made of voluminous continental flood basalts and many ultramafic–mafic–felsic intrusions (He et al., 2007; Shellnutt and Zhou, 2007; Xu et al., 2008, 2010; Shellnutt and Iizuka, 2011; Shellnutt et al., 2010, 2011; Zhong et al., 2011). Felsic intrusives (A-type granites, syenites, and I-type granites) in the Panxi area of Emeishan LIP show a wide variation in $\varepsilon_{Hf(t)}$ (−6.7 to +10.8, Xu et al., 2008; Zhong et al., 2011), similar to the range observed for the Group 2 samples ($\varepsilon_{Hf(t)}$ = −14.9 to +10.1, ~260 Ma portion) from Penglaitan. $\varepsilon_{Hf(t)}$ of ~260 Ma magmas are all positive (i.e., Taihe A-type granite, Miyi, Cida, and Baima; Xu et al., 2008; Zhong et al., 2011), except for the Ailanghe I-type granites which show negative $\varepsilon_{Hf(t)}$. However, this intrusion was emplaced at 252–256 Ma, significantly younger than the main stage of Emeishan volcanism. The fact that no age younger than 256 Ma is found in the Penglaitan case argues against a direct link of the Group 2 claystones with the felsic members of Emeishan LIP.

The disparate geochemical behavior of Hf, Th and Nb in zircon provides a potential scheme for the tectonic setting discrimination

Table 6
Mineralogy comparison between typical felsic ashes and Penglaitan samples.

	Typical felsic ashes	Penglaitan samples
Clay mineral	Illite and montmorillonite (45–100%), kaolinite (0–55%), chlorite (~5%)	Celadonite (27.3–59.6%), illite (0–39.8%), montmorillonite (6.2–29.9%)
Non-clay mineral	Quartz and feldspar (a few or rare)	Quartz (27.8–37.6%), anatase (0–0.6%)

of the host magma, as recently suggested by Yang et al. (2012). Nb in arc magmas is strongly depleted compare to that of within-plate magmas (Sun and McDonough, 1989; Pearce and Peat, 1995). It follows that the arc zircons possess lower Nb/Hf and higher Th/Nb than those from within-plate settings at a comparable degree of magmatic fractionation. Using Hf, Th and Nb in zircons from well known tectonic settings, Yang et al. (2012) were able to distinguish an extensional within-plate/anorogenic environment from a compressional magmatic arc/orogenic setting. The Group 2 zircons (~260 Ma portion) mostly fall in the orogenic (arc-related) field (Fig. 6c and d; Table 5). This again rules out the possibility that Group 2 samples are derived from the felsic part of Emeishan LIP. Therefore the source of the Group 2 sediments from Penglaitan is different from that of Wangpo bed in northern Sichuan. The latter was produced by erosion of the Emeishan LIP (He et al., 2007, 2010). Different sources for GLB claystones in different localities reinforced their terrigenous clastic origin, because in the case volcanic ashes, claystones from different areas would have essentially similar compositions.

Compiled with previously published U–Pb zircon age spectra, the analyses of detrital zircons in the Group 2 samples may help decipher the other two sources. The main U–Pb peak age of detrital zircons in Group 2 samples is 262 ± 3 Ma. Many geochronological studies have been carried out on the Cathaysia Block, but none produces ca. 262 Ma ages (e.g. Wang et al., 2007; Li et al., 2012). The data are therefore not consistent with the Cathaysia Block as the source of the Penglaitan Group 2 sediments. In contrast, the northern margin of Tethys had magmatic activities of similar ages. For instance, Li et al. (2006) dated calc-alkaline granites from Hainan Island and obtained an age of 267–262 Ma. There are massive magmatic activities at that time in the northern Vietnam (Lan et al., 2003; Hoa et al., 2008), which show an intermediate-felsic arc affinity. As shown in Fig. 3b, REE patterns of the Penglaitan Group 2 samples (PLT-2 to PLT-6) and of Hainan Island magmatic arc rocks are virtually identical. The Group 2 samples may share a common source with the arc-related magmatism. Moreover, the main age peak of 259–263 Ma is very close to age (260.4 ± 0.4 Ma, Gradstein et al., 2004) of the G/L boundary, suggesting that continental arc magmas were eroded, transported and deposited elsewhere quickly after their formation. Hf isotopic compositions of these ca. 260 Ma zircons (Table 4 and Fig. 5a) are consistent with a derivation from a source of old crustal sources mixed by newly mantle-derived melts, as would be expected in the case of an active continental margin. We thus propose that the Group 2 claystones may have been derived from continental arc rocks related to palaeo-Tethys evolution. If this interpretation is correct, it provides the first sedimentary evidence for the existence of northern marginal arc of Tethys.

6. Conclusions

Based on mineralogical, geochemical, zircon U–Pb and Hf isotopic analyses of G/L boundary claystones from the Penglaitan section, the following conclusions can be drawn:

(1) The Penglaitan claystones are clastic rocks rather than acidic tuffs or ashes as previously thought. Thus the Penglaitan claystones are not suitable for G/L boundary age determination.
(2) The Group 1 claystones which were collected below the G/L boundary are likely derived from a mafic source which is genetically related to the Emeishan LIP. This implies the synchroneity between the G/L mass extinction and eruption of Emeishan volcanism.
(3) The Group 2 samples collected above the G/L boundary are derived from a felsic source, which is likely related to palaeo-Tethys continental arc magmatism.

Acknowledgements

We would like to thank Shu-Zhong Shen and an anonymous reviewer for their critical and constructive comments. This research was supported by National Basic Research Program of China (973 Program: 2011CB808905, 2011CB808906), a Grant from the National Natural Science Foundation of China (41073045) and the CAS/SAFEA International Partnership Program for Creative Research Teams (KZCX2-YW-Q04-06). This is contribution No IS-1578 from GIGCAS.

References

Bowring, S.A., Erwin, D.H., Jin, Y.G., Martin, M.W., Davidek, K., Wang, W., 1998. U/Pb zircon geochronology and tempo of the end-Permian mass extinction. Science 280 (5366), 1039–1045.
Campbell, I.H., Czamanske, G.K., Fedorenko, V.A., Hill, R.I., Stepanov, V., 1992. Synchronism of the Siberian traps and the Permian–Triassic boundary. Science 258 (5089), 1760–1763.
Chen, Z.Q., George, A.D., Wang, W.R., 2009. Effects of Middle–Late Permian sea-level changes and mass extinction on the formation of the Tieqiao skeletal mound in the Laibin area, South China. Australian Journal of Earth Sciences 566, 745–763.
Chen, Z.Q., Jin, Y.G., Shi, G.R., 1998. Permian transgression–regression sequences and sea-level changes of South China. Proceedings of the Royal Society of Victoria 110, 345–367.
Condie, K.C., 1993. Chemical composition and evolution of the upper continental crust: contrasting results from surface samples and shales. Chemical Geology 104, 1–37.
Gradstein, F.M., Ogg, J.G., Simth, A.G., Bleeker, W., Lourens, L.J., 2004. A new geologic time scale, with special reference to Precambrian and Neogene. Episodes 272, 83–100.
Hallam, A., Wignall, P.B., 1999. Mass extinctions and sea-level changes. Earth-Science Reviews 48, 217–250.
Haq, B.U., Schutter, S.R., 2008. A chronology of Paleozoic sea-level changes. Science 322 (5898), 64–68.
Hayashi, K.I., Fujisawa, H., Holland, H.D., Ohmoto, H., 1997. Geochemistry of 1.9 Ga sedimentary rocks from northeastern Labrador, Canada. Geochimica et Cosmochimica Acta 61, 4115–4137.
He, B., Xu, Y.G., Huang, X.L., Luo, Z.Y., Shi, Y.R., Yang, Q.J., Yu, S.Y., 2007. Age and duration of the Emeishan flood volcanism, SW China: geochemistry and SHRIMP zircon U–Pb dating of silicic ignimbrites, post-volcanic Xuanwei Formation and clay tuff at the Chaotian section. Earth and Planetary Science Letters 255 (3–4), 306–323.
He, B., Xu, Y.G., Zhong, Y.T., Guan, J.P., 2010. The Guadalupian–Lopingian boundary mudstones at Chaotian (SW) China are clastic rocks rather than acidic tuffs: implication for a temporal coincidence between the end-Guadalupian mass extinction and the Emeishan volcanism. Lithos 119 (1–2), 10–19.
Hoa, T.T., Anh, T.T., Phuong, N.T., Dung, P.T., Anh, T.V., Izokh, A.E., Borisenko, A.S., Lan, C.Y., Chung, S.L., Lo, C.H., 2008. Permo-Triassic intermediate-felsic magmatism of the Truong Son belt, eastern margin of Indochina. Comptes Rendus Geoscience 340 (2–3), 112–126.

Isozaki, Y., 2003. Guadalupian–Lopingian boundary event in mid-Panthalassa: correlation of accreted deep-sea chert and mid-oceanic atoll carbonate. In: Wong, Th.E. (Eds.), Proceedings of the XVth International Congress on Carboniferous and Permian Stratigraphy. Utrecht, the Netherlands, 10–16 August 2003. Royal Netherlands Academy of Arts and Sciences.

Isozaki, Y., 2009a. Illawarra Reversal: the fingerprint of a superplume that triggered Pangean breakup and the end-Guadalupian Permian mass extinction. Gondwana Research 15 (3–4), 421–432.

Isozaki, Y., 2009b. Integrated "plume winter" scenario for the double-phased extinction during the Paleozoic–Mesozoic transition: the G–LB and P–TB events from a Panthalassan perspective. Journal of Asian Earth Science 36, 459–480.

Isozaki, Y., Yao, J.X., Matsuda, T., Sakai, H., Ji, Z.S., Shimizu, N., Kobayashi, N., Kawahata, H., Nishi, H., Takano, M., Kubo, T., 2004. Stratigraphy of the Middle–Upper Permian and Lowermost Triassic at Chaotian, Sichuan, China – record of end-Permian double mass extinction event. Proceedings of the Japan Academy B 80, 10–16.

Jin, Y.G., 1993. Pre-Lopingian benthos crisis. Comptes Rendus, XII ICC-P, Buenos Aires 2, 269–278.

Jin, Y.G., Shen, S.Z., Henderson, C.M., Wang, X.D., Wang, W., Wang, Y., Cao, C.Q., Shang, Q.H., 2006. The Global Stratotype Section and Point (GSSP) for the boundary between the Capitanian and Wuchiapingian stage Permian. Episodes 294, 253–262.

Jin, Y.G., Wang, Y., Wang, W., Shang, Q.H., Cao, C.Q., Erwin, D.H., 2000. Pattern of marine mass extinction near the Permian–Triassic boundary in South China. Science 289 (5478), 432–436.

Jin, Y.G., Zhang, J., Shang, Q.H., 1994. Two phases of the end-Permian mass extinction. In: Embry, A.F., Beauchamp, B., Glass, D.J. (Eds.), Pangea: Global Environments and Resources: Canadian Society of Petroleum Geologists, Memoir 17, pp. 813–822.

Jin, Y.G., Zhang, J., Shang, Q.H., 1995. Pre-Lopingian catastrophic event of marine faunas. Acta Palaeontologica Sinica 34, 410–427.

Kamo, S.L., Crowley, J., Bowring, S.A., 2006. The Permian–Triassic boundary event and eruption of the Siberian flood basalts: an inter-laboratory U–Pb dating study. Geochimica Et Cosmochimica Acta 7018. A303-A303.

Kamo, S.L., Czamanske, G.K., Amelin, Y., Fedorenko, V.A., Davis, D.W., Trofimov, V.R., 2003. Rapid eruption of Siberian flood-volcanic rocks and evidence for coincidence with the Permian–Triassic boundary and mass extinction at 251 Ma. Earth and Planetary Science Letters 214 (1–2), 75–91.

Kramer, W., Weatherall, G., Offler, R., 2001. Origin and correlation of tuffs in the Permian Newcastle and Wollombi Coal Measures, NSW, Australia, using chemical fingerprinting. International Journal of Coal Geology 47, 115–135.

Lan, C.Y., Chung, S.L., Hoa, T.T., Anh, T.T., 2003. Geochemical and Sr–Nd isotopic characteristics of Permo-Triassic arc magmatism, northern Vietnam. Research Abstracts 5, 03074.

Li, X.H., Li, Z.X., Zhou, H.W., Liu, Y., Kinny, P.D., 2002. U–Pb zircon geochronology, geochemistry and Nd isotopic study of Neoprozoic bimodal volcanic rocks in the Kangdian Rift of south China: implications for the initial rifting of Rodinia. Precambrian Research 113, 135–154.

Li, X.H., Li, Z.X., Li, W.X., Wang, Y.J., 2006. Initiation of the Indosinian Orogeny in South China: evidence for a Permian magmatic arc on Hainan Island. Journal of Geology 114 (3), 341–353.

Li, X.H., Li, Z.X., He, B., Li, W.X., Li, Q.L., Gao, Y.Y., Wang, X.C., 2012. The early Permian active continental margin and crustal growth of the Cathaysia Block: in situ U-Pb, Lu–Hf and O isotope analyses of detrital zircons. Chemical Geology 328, 195–207.

McLennan, S.M., Hemming, S., McDaniel, D.K., Hanson, G.N., 1993. Geochemical approaches to sedimentation, provenance and tectonics. Geological Society of America Special Paper 284, 21–40.

Metcalfe, I., Nicoll, R.S., Mundil, R., Foster, C., Glen, J., Lyons, J., Wang, X.F., Wang, C.Y., Renne, P.R., Black, L., Qu, X., Mao, X.D., 2001. The Permian–Triassic boundary and mass extinction in China. Episodes 244, 239–244.

Mundil, R., Ludwig, K.R., Metcalfe, I., Renne, P.R., 2004. Age and timing of the Permian mass extinctions: U/Pb dating of closed-system zircons. Science 305 (5691), 1760–1763.

Mundil, R., Metcalfe, I., Ludwig, K.R., Renne, P.R., Oberli, F., Nicoll, R.S., 2001. Timing of the Permian–Triassic biotic crisis: implications from new zircon U/Pb age data and their limitations. Earth and Planetary Science Letters 187 (1–2), 131–145.

Pearce, J.A., Peat, D.W., 1995. Tectonic implications of the composition of volcanic arc magmas. Annual Review of Earth and Planetary Sciences 23, 251–285.

Renne, P.R., Zhang, Z.C., Richards, M.A., Black, M.T., Basu, A.R., 1995. Synchrony and causal relations between Permian–Triassic boundary crises and Siberian flood volcanism. Science 269 (5229), 1413–1416.

Ross, C.A., Ross, J.R.P., 1987. Late Paleozoic sea-levels and depostitional sequence. In: Ross, C.A., Haman, D. (Eds.), Timing and Depositional History of Eustatic Sequences: Constraints on Seismic Stratigraphy. Cushman Foundation for Foraminiferal Research Special, Publication 24, pp. 137–149.

Ross, C.A., Ross, J.R.P., 1994. Permian sequence stratigraphy and fossil zonation. In: Beauchamp, B., Embry, A., Glass, D. (Eds.), Pangea: Global Environments and Resources. Canadian Society of Petroleum Geologists, Memoir 17, pp. 219–231.

Sha, Q., Wu, W., Fu, J., 1990. An Integrated Investigation on the Permian System of Qian-Gui Areas, with Discussion on the Hydrocarbon Potential. Science Press, Beijing.

Shellnutt, J.G., Iizuka, Y., 2011. Mineralogy from three peralkaline granitic plutons of the Late Permian Emeishan large igneous province (SW China): evidence for contrasting magmatic conditions of A-type granitoids. European Journal of Mineralogy 23 (1), 45–61.

Shellnutt, J.G., Jahn, B.M., Dostal, J., 2010. Elemental and Sr–Nd isotope geochemistry of microgranular enclaves from peralkaline A-type granitic plutons of the Emeishan large igneous province, SW China. Lithos 119 (1–2), 34–46.

Shellnutt, J.G., Jahn, B.M., Zhou, M.F., 2011. Crustally-derived granites in the Panzhihua region, SW China: implications for felsic magmatism in the Emeishan large igneous province. Lithos 123 (1–4), 145–157.

Shellnutt, J.G., Zhou, M.F., 2007. Permian peralkaline, peraluminous and metaluminous A-type granites in the Panxi district, SW China: their relationship to the Emeishan mantle plume. Chemical Geology 243, 286–316.

Shen, S.Z., Crowley, J.L., Wang, Y., Bowring, S.A., Erwin, D.H., Sadler, P.M., Cao, C.Q., et al., 2011. Calibrating the End-Permian mass extinction. Science 334, 1367–1372.

Shen, S.Z., Shi, G.R., 1996. Diversity and extinction patterns of Permian Brachiopoda of South China. Historical Biology 12, 93–110.

Shen, S.Z., Shi, G.R., 2002. Paleobiogeographical extinction patterns of Permian brachiopods in the Asian-western Pacific region. Paleobiology 28, 449–463.

Shen, S.Z., Wang, Y., Henderson, C.M., Cao, C.Q., Wang, W., 2007. Biostratigraphy and lithofacies of the Permian System in the Laibin-Heshan area of Guangxi, South China. Palaeoworld 16(1–3), 120–139 (Sp. Iss. Sl).

Spears, D.A., Kanaris-Sotiriou, R., 1979. A geochemical and mineralogical investigation of some British and other European tonsteins. Sedimentology 26, 407–425.

Stanley, S.M., Yang, X., 1994. A double mass extinction at the end of the Paleozoic era. Science 266 (5189), 1340–1344.

Sun, S.S., McDonough, W.F., 1989. Chemical and isotopic systematics of oceanic basalts: implications for mantle composition and processes. In: Saunders, A.D., Norry, M.J. (Eds.), Magmatism in Ocean Basins. Geological Society of London Special Publication, v. 42, pp. 313–345.

Taylor, S.R., McLennan, S.M., 1985. The Continental Crust: Its Composition and Evolution. Blackwell Scientific Publications, Blackwell, Oxford, UK, 312 pp.

Wang, W., Cao, C.Q., Wang, Y., 2004. The carbon isotope excursion on (GSSP) candidate section of Lopingian–Guadalupian boundary. Earth and Planetary Science Letters 220 (1–2), 57–67.

Wang, X.D., Sugiyama, T., 2000. Diversity and extinction patterns of Permian coral faunas of China. Lethaia 33, 285–294.

Wang, Y., Jin, Y.G., 2000. Permian palaeogeographic evolution of the Jiangnan Basin, South China. Palaeogeography Palaeoclimatology Palaeoecology 160 (1–2), 35–44.

Wang, Y.J., Fan, W.M., Zhao, G.C., Ji, S.C., Peng, T.P., 2007. Zircon U–Pb geochronology of gneissic rocks in the Yunkai massif and its implications on the Caledonian event in the South China Block. Gondwana Research 12 (4), 404–416.

Weidlich, O., Kiessling, W., Flugel, E., 2003. Permian–Triassic boundary interval as a model for forcing marine ecosystem collapse by long-term atmospheric oxygen drop. Geology 31 (11), 961–964.

Wignall, P.B., Sun, Y.D., Bond, D.P.G., Izon, G., Newton, R.J., Védrine, S., Widdowson, M., Ali, J.R., Lai, X.L., Jiang, H.S., Cope, H., Bottrell, S.H., 2009a. Volcanism, mass extinction, and carbon isotope fluctuations in the Middle Permian of China. Science 324 (5931), 1179–1182.

Wignall, P.B., Védrine, S., Bond, D.P.G., Wang, W., Lai, X.L., Ali, J.R., Jiang, H.S., 2009b. Facies analysis and sea-level change at the Guadalupian–Lopingian Global Stratotype Laibin, South China, and its bearing on the end-Guadalupian mass extinction. Journal of the Geological Society 166, 655–666.

Wu, F.Y., Yang, Y.H., Xie, L.W., Yang, J.H., Xu, P., 2006. Hf isotopic compositions of the standard zircons and baddeleyites used in U–Pb geochronology. Chemical Geology 234, 105–126.

Xiao, L., Xu, Y.G., Mei, H.J., Zheng, Y.F., He, B., Pirajno, F., 2004. Distinct mantle sources of low-Ti and high-Ti basalts from the western Emeishan large igneous province, SW China: implications for plume-lithosphere interaction. Earth and Planetary Science Letters 228, 525–546.

Xu, Y.G., Chung, S.L., Shao, H., He, B., 2010. Silicic magmas from the Emeishan large igneous province, Southwest China: petrogenesis and their link with the end-Guadalupian biological crisis. Lithos 119 (1–2), 47–60.

Xu, Y.G., Luo, Z.Y., Huang, X.L., He, B., Xiao, L., Xie, L.W., Shi, Y.R., 2008. Zircon U–Pb and Hf isotope constraints on crustal melting associated with the Emeishan mantle plume. Geochimica et Cosmochimica Acta 72 (13), 3084–3104.

Yang, J.H., Cawood, P.A., Du, Y.S., Huang, H., Huang, H.W., Tao, P., 2012. Large Igneous Province and magmatic arc sourced Permian–Triassic volcanogenic sediments in China. Sedimentary Geology 261–262, 120–131.

Yang, Z.Y., Shen, W.Z., Zheng, L.D., 2009. Elements and isotopic geochemistry of Guadalupian-Lopingian boundary profile at the Penglaitan Section of Laibin, Guangxi Province, and Its geological implications. Acta Geologica Sinica 83, 1–15 (in Chinese with English abstract).

Yin, H.F., Huang, S.J., Zhang, K.X., Yang, F.Q., Ding, M.H., Bi, X.M., Zhang, S.X., 1989. Volcanism at the Permian–Triassic Boundary in South China and its effects on mass extinction. Acta Geologica Sinica 63 (2), 169–180 (in Chinese with English abstract).

Yin, H.F., Zhang, K.X., Tong, J.N., Yang, Z.Y., Wu, S.B., 2001. The Global Stratotype Section and Point (GSSP) of the Permian–Triassic boundary. Episodes 242, 102–114.

Zhang, S.X., Yu, J.X., Yang, F.Q., Peng, Y.Q., Yin, H.F., Yu, J.S., 2004. Study on clayrocks of the neritic, littoral and marine-terrigenous facies across the Permian–Triassic boundary in the eastern Yunnan and western Guizhou, South China. Journal of Mineralogy and Petrology 24 (4), 81–86 (in Chinese with English abstract).

Zhang, S.X., Feng, Q.L., Gu, S.Z., Yu, J.S., 2006a. Claystone around deep water Permian–Triassic boundary from Guizhou and Guangxi reigon. Geological Science and Technology Information 25 (1), 9–13 (in Chinese with English abstract).

Zhang, S.X., Peng, Y.Q., Yu, J.X., Lei, X.R., Gao, Y.Q., 2006b. Characteristics of claystones across the terrestrial Permian–Triassic boundary: evidence from the Chahe section, western Guizhou, South China. Journal of Asian Earth Sciences 27 (3), 358–370.

Zhong, H., Campbell, I.H., Zhu, W.G., Allen, C.M., Hu, R.Z., Xie, L.W., He, D.F., 2011. Timing and source constraints on the relationship between mafic and felsic intrusions in the Emeishan large igneous province. Geochimica et Cosmochimica Acta 75, 1374–1395.

Zhou, L., Kyte, F.T., 1988. The Permian–Triassic boundary event – a geochemical study of 3 Chinese sections. Earth and Planetary Science Letters 904, 411–421.

Zhou, M.F., Malpas, J., Song, X.Y., Robinson, P.T., Sun, M., Kennedy, A.K., Lesher, C.M., Keays, R.R., 2002. A temporal link between the Emeishan large igneous province SW China and the end-Guadalupian mass extinction. Earth and Planetary Science Letters 196, 113–122.

Zhou, Y.P., Ren, Y.L., Bohor, B.F., 1982. Origin and distribution of tonsteins in Late Permian coal seams of southwestern China. International Journal of Coal Geology 2, 49–77.